The Journal of Nutritional Biochemistry

Hepatic metabolic adaptation and adipose tissue expansion are altered in mice with steatohepatitis induced by high-fat high sucrose diet

--Manuscript Draft--

Manuscript Number:	JNB_2020_299R1
Article Type:	Research Paper
Keywords:	NAFLD; Adipose tissue; Autophagy; sucrose.; Obesity
Corresponding Author:	Jordi Camps Hospital Universitari de Sant Joan Reus, Spain
First Author:	Gerard Baiges-Gaya
Order of Authors:	Gerard Baiges-Gaya
	Salvador Fernández-Arroyo
	Fedra Luciano-Mateo
	Noemí Cabré
	Elisabet Rodríguez-Tomàs
	Anna Hernández-Aguilera
	Helena Castañé
	Marta Romeu
	M. Rosa Nogues
	Jordi Camps
	Jorge Joven
Abstract:	Background: Obesity is a chronic progressive disease with several metabolic alterations. Non-alcoholic fatty liver disease (NAFLD) is an important co-morbidity of obesity that can progress to non-alcoholic steatohepatitis (NASH), cirrhosis or hepatocarcinoma. This study aimed at clarifying the molecular mechanisms underlying the metabolic alterations in hepatic and adipose tissue during high-fat high-sucrose diet-induced NAFLD development in mice. Methods: Twenty-four male mice (C57BL/6J) were randomly allocated into 3 groups (n=8 mice per group) to receive a chow diet, a high-fat diet (HFD), or a high-fat high-sucrose diet (HF-HSD) for 20 weeks. At sacrifice, liver and adipose tissue were obtained for histopathological, metabolomic, and protein expression analyses. Results: HF-HSD (but not HFD) was associated with NASH and increased oxidative stress. These animals presented an inhibition of hepatic autophagy and alterations in AMP-activated protein kinase/mammalian target of rapamycin activity. We also observed that the ability of metabolic adaptation was adversely affected by the increase of damaged mitochondria. NASH development was associated with changes in adipose tissue dynamics and increased amounts of saturated fatty acids, monounsaturated fatty acids and polyunsaturated fatty acids in visceral adipose tissue. Conclusion: HF-HSD led to a metabolic blockage and impaired hepatic mitochondria turnover. In addition, the continuous accumulation of fatty acids produced adipose tissue dysfunction and hepatic fat accumulation that favored the progression to NASH.
Suggested Reviewers:	Shanthi Srinivasan ssrini2@emory.edu
	Frank Tacke frank.tacke@gmx.net
	amalia gastaldelli amalia@ifc.cnr.it
	Stergios Polyzos

	spolyzos@auth.gr
	Hayato Nakagawa hanakagawa-tky@umin.ac.jp
Response to Reviewers:	

Dr. Bernhard Hennig, Editor-in-Chief
The Journal of Nutritional Biochemistry
University of Kentucky
900 Limestone Street
Rm. 599, Wethington Health Sciences Building
Lexington, KY 40536-0200
USA
Ref.: Ms. # JNB_2020_299

Reus, June 23, 2020

Dear Dr. Hennig,
Thank you very much for giving us the opportunity to resumbit our article entitled *"Hepatic metabolic adaptation and adipose tissue expansion are altered in mice with steatohepatitis induced by high-fat high sucrose diet"*. We have taken into account all the Reviewers' suggestions, and the itemized answers are in the accompanying files.

We hope the manuscript is now acceptable for publication in the Journal of Nutritional Biochemistry.

Sincerely yours,
Dr. Jordi Camps
Corresponding author

REVISION NOTE
Journal of Nutritional Biochemistry
Ms. # JNB_2020_299

Reviewer #1:

Comment #1: *«In the manuscript JNB_2020_299, Baiges-Gaya et al studied high-fat diet and high-fat high-sucrose diet induced changes in the liver and adipose tissues. The metabolic changes in mice were not surprising or new, and this paper is potentially important if the mechanisms are properly addressed. However, the data presented in the present version of the manuscript is insufficient and needs additional work to strengthen its scientific merits as described below: (1) autophagy flux activities should be measured in the present and absence of bafilomycin A1 and CQ. Current data only showed the steady state level of p62 and LC3, known to be insufficient to characterize autophagy activity».*
Response: We thank the Reviewer for these constructive comments and good ideas for improving the manuscript. Unfortunately, the laboratories of our Institution are partially closed due to the pandemic afflicting our country and the rest of the World and, although we are able of doing some analyses, we cannot foresee when we will be able to carry out new sets of complex experiments. We take into account the Reviewer's suggestion for future studies when possible. In this revised version we have deleted the term autophagy from the title, downgraded the interpretation of our results and added a sentence as a limitation of the study (lines 349-357 and 519-522).

Comment #2: *«Fig 3C: bar graph for pACC/ACC should be presented; Fig 4B: bar graphs and statistics should be presented for all phosphorylated proteins/total proteins; Fig 5D: bar graphs and statistics should be presented for the western blot data as in Figs 3-4».*
Response: We have modified these figures as requested.

Comment #3: *«Fig 3C: C2-C5 proteins were downregulated by HFD or HFHSD, which was inconsistent with the authors' claim of inhibited autophagy/mitophagy».*
Response: This is a debatable issue. For example, a recent study in mice with NAFLD *(doi: 10.1074/mcp.RA118.000961)* reported that, as the Reviewer indicates, a decrease in oxidative phosphorylation proteins was associated with an increase in some mitophagy markers. However, the same study found that proteasomal degradation activity was reduced, suggesting that *"ATP deficiency because of reduced stability of oxidative phosphorylation complex subunits contributed to inhibition of ubiquitin-proteasome and activation of mitophagy"*. Moreover, another study in mice fed with a high-fat diet showed an increase in the activities of complex I and complex II and an increase in ATP production *(*doi: *10.1074/mcp.M113.027441)*. On the other hand, there are some reports indicating that complexes I and III are required to normal autophagy flux and their suppression led to autophagy inhibition *(doi.org/10.1016/j.celrep.2018.07.101; doi: 10.1111/j.1471-4159.1990.tb02325.x; doi.org/10.1016/j.chembiol.2011.08.009, doi.org/10.1016/j.chembiol.2011.11.004)*. Moreover, the inhibition of Complex V with oligomycin has been reported to promote mitochondrial dysfunction and death in cell cultures *(*doi.org/10.1002/art.39025*)*, and in Alzheimer disease, the low expression of CI, CII, CIII, CIV and CV was associated with a mitophagy failure *(doi:10.1007/s12035-019-01665-y)*. All these data support our results in the HF-HSD group, which show a downregulation of CII, CIII and CV, associated with reduction of autophagy/mitophagy. Results obtained to-date can be open to more than one interpretation, and different diets or different weeks of treatment make difficult to reach a consensus.

Comment #4: *«Please consider using a scheme to picture the new mechanism revealed by this study».*
Response: We are sorry. A general scheme could be made by modifying figure 4A, but as a consequence of a request from Reviewer #2, this figure has been deleted.

Comment #5: *«UCP1 per se does not oxidize fat».*
Response: We have modified this sentence (lines 371-374).

Comment #6: *«VAT per se is not an ectopic fat-storing tissue. The related statements should be corrected».*
Response: We have modified these statements (lines 95-98).

Comment #7: *«In addition, literature review was insufficient in the Introduction: current issue(s) and why this present study was significant were not properly addressed».*
Response: We agree with the Reviewer suggestion. We have updated the Introduction accordingly and added some new references (lines 98 –104, ref. #12-14).

Reviewer #2:

General comment: *«The manuscript examines the differential effects of a high fat diet (HFD) and a high fat, high sucrose diet HFHSD) on changes in various metabolic pathways in the liver and adipose tissue in mice and their ability to induce nonalcoholic steatohepatitis (NASH). The study reveals the different metabolic pathways in the liver that can be impacted in NAFLD. The authors report increased steatosis, hepatocyte ballooning and the presence of markers of inflammation indicative of NASH in HFHSD-fed mice, but not HFD-fed mice. They also report reductions in the hepatic expression of enzymes involved in the breakdown of reactive oxygen species, and an increase in the expression of markers of tissue oxidative stress. They observed reductions in the levels of proteins of the mitochondrial electron transport chain in liver from HFHSD-fed mice and increase in the levels of LC3II and p62/SQSTM1 indicative of impaired autophagy. In addition, they observed increased liver levels Pink1, parkin and mitofusin 2. While interesting, the manuscript several major issues need to be addressed as mentioned below».*
Response: We thank the Reviewer for all these comments. In the following sections we have tried to give a point by point answer to all of them.

Comment #1: *«The data presented in this manuscript does not show unequivocally that steatohepatitis results from mitochondrial damage. Hence, the title is misleading. The link between the diet and mitochondrial damage was not established in the manuscript».*
Response: We agree with the Reviewer criticism. We have modified the title accordingly.

Comment #2: *«In addition to the metabolomic data it would have been helpful if gene expression analyses were performed. They probably could have revealed more differences between the diets».*
Response: This is an interesting suggestion. In this revised manuscript, we have analyzed the gene expression of ATP citrate lyase (ACLY), isocitrate dehydrogenase 1 (IDH1), isocitrate dehydrogenase 2 (IDH2), alpha-ketoglutarate dehydrogenase (OGDH), and succinate dehydrogenase (SDHA). The results obtained showed that HF-HSD mice had a higher increase expression of ACLY and IDH2, which indicates a change of metabolic flux towards lipogenesis (lines 259-270 and 339-343, Figure 3).

Comment #3: *«The catalog numbers for the diets were not provided making it difficult to compare the results of this study with others».*
Response: We have added the catalog numbers (lines 122-125).

Comment #4: *«In the methods section under immunoblotting it is not indicated if loading controls such as beta actin or alpha tubulin were used and how differences in band densities were assessed».*
Response: We used FAH as a loading control. We have added the requested information (lines 254-256).

Comment #5: *«Description of how metabolites and lipids were assessed are included in the statistics section while they should have been in the appropriate method section».*

Response: We have done the suggested change (lines 220 -227).

Comment #6: *«While several illustrations (Fig. 3A-B) and 4A)) have been used to pinpoint the specific proteins altered by the different diets, simple tables listing these proteins and the pathways they are involved in would have made the manuscript easier to follow. The illustrations would fit in well as supplementary data».*

Response: We accept the reviewer's criticism. The information shown in figure 3A-B of the original manuscript is now indicated in Table 1, while the Figure has been moved to Supplementary Information (line 327). We have not turned Figure 4A into a Table because it does not refer to any analytical measurement and, taking into account the Reviewer's comment, we have decided to delete it.

Comment #7: *«Fig. 1 A-C the key symbols do not match the symbols used in the curves thus making it hard to tell which curves represent which group».*

Response: We have done the suggested change (Figure 1).

Comment #8: *«Fig. 1D fasting blood glucose levels for control mice fed Chow diet are too high. One would expect readings not exceeding 150 mg/ml. It is possible tha samples were greatly hemolyzed. One would also have expected larger differences in triglyceride values».*

Response: The Reviewer is absolutely right. We have repeated the analyses and the results are shown in the new figure 1. We apologize for our mistake (Figure 1).

Comment #9: *«1E. Lower magnification H&E images would have been preferable to show a larger area».*

Response: We have done the suggested change and the new images are shown in the Figure 1

Comment #10: *«1.F. Steatosis, ballooning and inflammation scores should have been presented in tabular form or as scattergram (dot plots) for easy interpretation of data. Also, there is no indication in the materials and methods if the scoring was performed randomly or if it was performed by an expert pathologist».*

Response: We accept the reviewer's criticism. We have done the suggested changes (lines 139 and Figure 1).

Comment #11: «*Fig. 1 Why wasn't collagen staining performed too?».*

Response: We examined collagen content using the Sirius red staining, but found no accumulation of fibrosis in any of the dietary groups and decided not to include these results in the manuscript because we think they do not provide any relevant information. The graphics below are for the Reviewer's information.

Control **HFD** **HF-HSD**

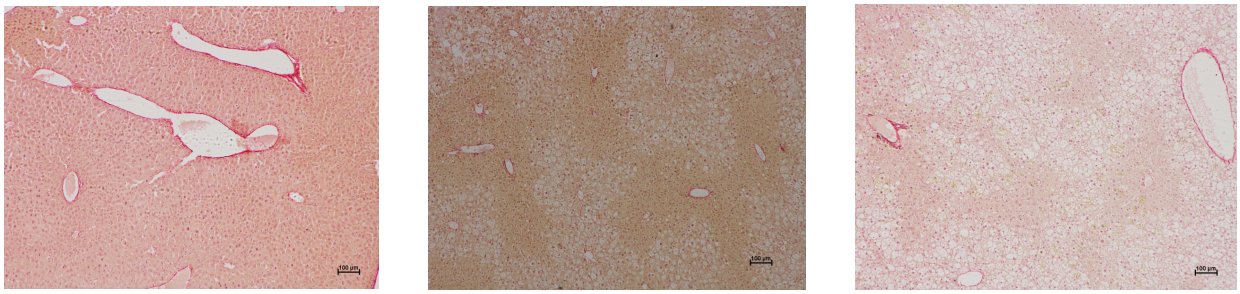

Comment #12: *«Fig.2. Western blotting for phospho junk and phospho c-jun would further confirm the existence of tissue oxidative stress».*

Response: This is an interesting suggestion. In this revised version, we performed western blotting of c-Jun and phospho-c-Jun and the results showed an activation of c-Jun (Ser73) in mice fed HF-HSD, corroborating our results (lines 307-309, Figure 2C).

Comment #13: *«Fig. 3C, 4B, 5D.and S1. The way the gel bands are presented makes it look like samples from the different diet groups were run on separate gels which would be unacceptable. No loading controls were included in the Westerns».*

Response: We have presented the cropped western blots for clarity. However, we have taken into account the Reviewer's criticism and, in this revised version, we have added the uncropped blots as Additional Suporting Information. We use FAH as a loading control (lines 254-256). (https://doi.org/10.1038/s41590-019-0372-7; https://doi.org/10.1016/j.bbadis.2019.03.006; https://doi.org/10.1016/j.metabol.2019.07.002)

Comment #14: *«Fig. 4. Are increased in hepatic levels of pink1, parkin1 and mitofusin-2 indicative of impaired mitophagy? Several in vitro studies show reduced levels of these proteins in hepatocytes exposed to the saturated fatty acid palmitate. Ideally, immunofluorescence staining for these proteins and seeing if they colocalize with markers of mitochondria and autophagy would have helped to show if these is impaired mitophagy».*

Response: This is a very interesting comment. The presence of PINK1 and PARKIN is necessary for the ubiquitination of various substrates and the formation of the ubiquitin chain (activation of mitophagy). In our results, we observed that the HF-HSD group showed high levels of PINK1 and PARKIN, suggesting the activation of mitophagy due to mitochondrial damage. However, damaged ubiquitinated mitochondria must be recruited by phagophores to allow fusion with the lysosome to degrade. At this level, we observed an increase in the ubiquitin-associated protein P62 and LC3 II, which breaks down in autolysosomes, indicating an accumulation of autophagosomes waiting to be degraded. Then, in the HFHSD group, the autophagy and mitophagy machinery were started, but the accumulation of the levels of LC3II and P62 suggests a deterioration of the fusion of phagophores with the lysosome. This point has been commented in the revised version of our manuscript (lines 358-364). We agree that it would have been very interesting to perform immunofluorescence staining for these proteins, but we do not have the appropriate microscope.

Comment #15: *«Fig. 5 A and B. Can the authors highlight why this data is included in the manuscript. It is expected that there would be increased fat accumulation in white adipose tissue in HFD and HF-HSD-fed mice when compared to CD-fed mice. Fig. 5D. Comparison of band densities is not provided making it hard to draw any conclusions».*

Response: As you say, the relationship between adipocyte size (hypertrophy) and obesity is widely known. However, the mechanisms that regulate adipocyte size remain poorly understood. Considering that we used two different types of hypercaloric diet and that the animal responses were different, we considered necessary to explore the capacity of adipose tissue expansion, which is related to insulin sensitivity. Moreover, the size of adipocyte not always it is a well indicator of dysfunction. Indeed, some disease such as lipodystrophy shows a limited adipose tissue expansion and present metabolic disorders as NAFLD, indicating that the function of adipose tissue is more important than adiposity.
In relation to Fig.5D. we have done the suggested change.

Highlights

- High-fat high-sucrose diets (HF-HSD) promote NAFLD and NASH in mice
- HF-HSD is associated with oxidative stress and inhibition of hepatic autophagy
- HF-HSD produces metabolic inflexibility associated with mitochondrial damage
- NASH is related to changes in adipose tissue dynamics and fatty acid accumulation

Graphical abstract

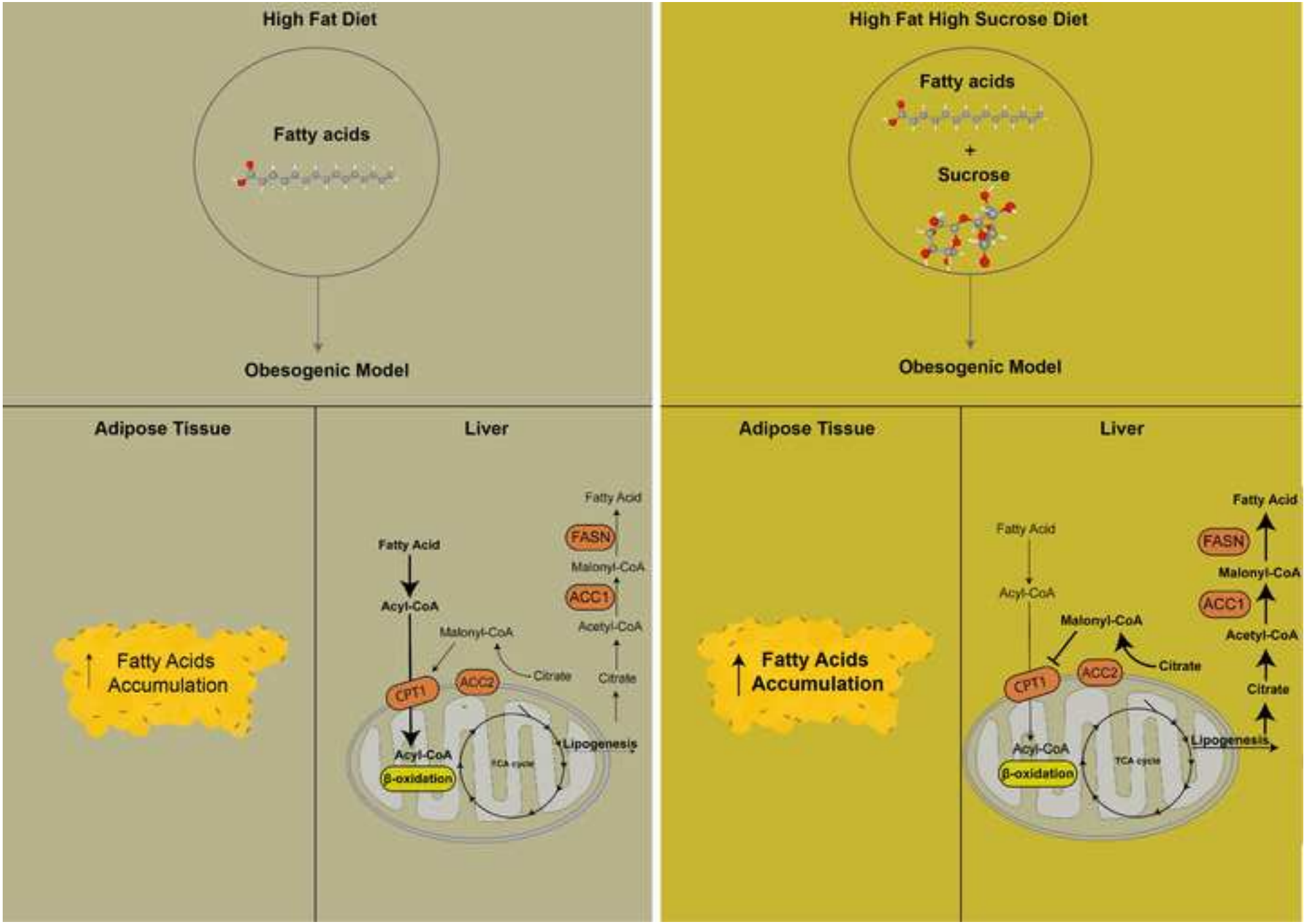

Hepatic metabolic adaptation and adipose tissue expansion are altered in mice with steatohepatitis induced by high-fat high sucrose diet

Gerard Baiges-Gaya[a,b], Salvador Fernández-Arroyo[a,b] Fedra Luciano-Mateo[a,b], Noemí Cabré[a,b], Elisabet Rodríguez-Tomàs[a,b], Anna Hernández-Aguilera[a,b], Helena Castañé[a,b], Marta Romeu[c], Maria-Rosa Nogués[c], Jordi Camps[a,b,*], Jorge Joven[a,b,d,*]

[a] *Universitat Rovira i Virgili, Departament de Medicina i Cirurgia, Facultat de Medicina, Reus, Spain*

[b] *Unitat de Recerca Biomèdica, Hospital Universitari de Sant Joan, Institut d'investigació Sanitària Pere Virgili, Reus, Spain*

[c] *Universitat Rovira i Virgili, Departament de Ciències Mèdiques Bàsiques, Facultat de Medicina, Unitat de Farmacologia, Reus, Spain*

[d] *Campus of International Excellence Southern Catalonia, Tarragona, Spain*

*Corresponding authors at: Unitat de Recerca Biomèdica, Hospital Universitari de Sant Joan, C. Sant Joan s/n, 43201 Reus, Spain

E-mail addresses: jcamps@grupsagessa.com (J. Camps) or jjoven@grupsagessa.com (J. Joven).

Email addresses:

GBG: gerard.baiges@iispv.cat; SFA: salvador.fernandezarroyo@gmail.com; FLM: fedra.luciano@gmail.com ; NC: ncabre@scripps.edu; ERT: elisabet.rodriguez@urv.cat; AHA: anna.hernandeza@gmail.com; HC: helena.castanev@gmail.com; MR: marta.romeu@urv.cat; MRN: mariarosa.nogues@urv.cat; JC: jcamps@grupsagessa.com; JJ: jjoven@grupsagessa.com.

Running Title: NASH and diet-induced metabolic alterations in mice

ABSTRACT

Background: Obesity is a chronic progressive disease with several metabolic alterations. Non-alcoholic fatty liver disease (NAFLD) is an important co-morbidity of obesity that can progress to non-alcoholic steatohepatitis (NASH), cirrhosis or hepatocarcinoma. This study aimed at clarifying the molecular mechanisms underlying the metabolic alterations in hepatic and adipose tissue during high-fat high-sucrose diet-induced NAFLD development in mice.

Methods: Twenty-four male mice (C57BL/6J) were randomly allocated into 3 groups (n=8 mice per group) to receive a chow diet, a high-fat diet (HFD), or a high-fat high-sucrose diet (HF-HSD) for 20 weeks. At sacrifice, liver and adipose tissue were obtained for histopathological, metabolomic, and protein expression analyses.

Results: HF-HSD (but not HFD) was associated with NASH and increased oxidative stress. These animals presented an inhibition of hepatic autophagy and alterations in AMP-activated protein kinase/mammalian target of rapamycin activity. We also observed that the ability of metabolic adaptation was adversely affected by the increase of damaged mitochondria. NASH development was associated with changes in adipose tissue dynamics and increased amounts of saturated fatty acids, monounsaturated fatty acids and polyunsaturated fatty acids in visceral adipose tissue.

Conclusion: HF-HSD led to a metabolic blockage and impaired hepatic mitochondria turnover. In addition, the continuous accumulation of fatty acids produced adipose tissue dysfunction and hepatic fat accumulation that favored the progression to NASH.

[Abstract word count: 216]

Keywords: Adipose tissue; autophagy; NAFLD; NASH; obesity; sucrose

54 **Abbreviations:**

55 4-HNE, 4-hydroxy-2-nonenal; ACC1, acetyl-CoA carboxylase 1; ACC2, acetyl-CoA
56 carboxylase 2; ACLY, ATP citrate-lyase; AMPK, AMP-activated protein kinase; ATG7,
57 autophagy-related protein 7; CA, cholic acid; CAC, citric acid cycle; CAT, catalase; CCL2,
58 chemokine (C-C motif) ligand 2; CD, chow diet; CD11b, cluster of differentiation 11b;
59 CD163, cluster of differentiation 163; CLEC4F, c-type lectin domain family 4; c-Jun, Jun
60 proto-oncogene; DNL, de novo lipogenesis; F4/80, EGF-like module-containing mucin-
61 like hormone receptor-like 1; FAH, fumarylacetoacetate hydrolase; FAO, fatty acid
62 oxidation; FASN, fatty acid synthase; FRAP, ferric ion reducing antioxidant power; GPx,
63 glutathione peroxidase; GR, glutathione reductase; HFD, high fat diet; HSL, hormone
64 sensitive lipase; HF-HSD, high-fat high-sucrose diet; IDH, Isocitrate dehydrogenase;
65 iWAT; inguinal white adipose tissue; LC3B, microtubule-associated proteins 1A/1B light
66 chain 3B; MAPK, mitogen activated protein kinase; MFN2, mitofusin 2; mTOR,
67 mammalian target of rapamycin; NAFLD, non-alcoholic fatty liver disease; NASH, non-
68 alcoholic steatohepatitis; OGDH; oxoglutarate dehydrogenase; P62, sequestosome 1;
69 PARKIN, E3 ubiquitin- protein ligase parkin; pgWAT, perigonadal white adipose tissue;
70 PINK1, PTEN-induced putative kinase 1; PLSDA, partial least squares discriminant
71 analysis; PON1, paraoxonase 1; PPP, pentose phosphate pathway; PUFA,
72 polyunsaturated fatty acids; SAT, subcutaneous adipose tissue; SDHA, succinate
73 dehydrogenase, SOD, superoxide dismutase; SFA, saturated fatty acids; TNFα, tumor
74 necrosis factor-α; TOM20, translocase outer membrane 20; UCP-1, uncoupling protein
75 1; VAT, visceral adipose tissue; VIP, variable importance in projection; WAT, white
76 adipose tissue.

77 **1. Introduction**

78 The prevalence of obesity has increased in recent decades and this
79 phenomenon constitutes a serious health problem worldwide [1]. Non-alcoholic fatty
80 liver disease (NAFLD) is an important co-morbidity of obesity. The most severe form of
81 NAFLD is non-alcoholic steatohepatitis (NASH) which, currently, represents the main
82 reason for liver transplantation [2]. Abnormal nutrient intake is a fundamental
83 contributor to obesity and the related metabolic liver disease. Several studies linked
84 the consumption of fat and sugars with the development of obesity [3,4]. However,
85 the molecular mechanisms that can explain these effects of diets are poorly
86 understood. The complex interactions between the liver and adipose tissue makes
87 necessary the study NAFLD from a global metabolic perspective [5,6] since these
88 organs are involved in the regulation of whole-body energy homeostasis, and have a
89 great capacity of adaptation to metabolic needs. An excessive nutrient intake
90 promotes triglyceride storage and, thereby, an increase in adipocyte size of white
91 adipose tissue (WAT) while maintaining homeostasis. However, there is a large
92 variation in adipocyte metabolism within and between individuals [7–9]. Subcutaneous
93 adipose tissue (SAT) represents around 80% of WAT and constitutes the main reservoir
94 of lipid storage. The magnitude of adiposity is influenced by the growth potential of
95 adipose cells and their ability to induce turnover of triglycerides [10,11]. Indeed, when
96 the ability of SAT to release fatty acids is reduced, accumulation of fat in visceral
97 adipose tissue (VAT) and ectopic fat deposition on metabolic organs such as liver or
98 muscle may occur [10]. Moreover, it has been reported in both humans and animal
99 models that the dysfunction of adipose tissue lead to metabolic inflexibility [12-14]. As
100 a result, large visceral fat cells are produced, and the liver captures excess circulating
101 fatty acids leading to an increase in hepatic fat accumulation which can produce an
102 inflammatory response [15]. The accumulation of defective mitochondria and
103 malfunctioning cytoplasmatic protein progressively increases which results in
104 autophagy suppression and progression to steatohepatitis [16,17].

105 In this study, we investigated the differences physiological and metabolic
106 implicated on NAFLD development and alterations of adipose tissue caused by two

107 different types of western diets, supporting the concept that the dietetic pattern
108 established it is decisive point in the impaired metabolic flexibility.
109

110 **2. Methods**

111 *2.1. Animal care and diets*

112 All experiments were performed in compliance with the guidelines established
113 by the Committee on Animal Care of the *Universitat Rovira i Virgili* and conform to the
114 Animal Research: Reporting of *In Vivo* Experiments (ARRIVE) guidelines. Four-week-old
115 male mice (C57BL/6J) were obtained from Charles River Laboratories (Wilmington, MA,
116 USA) and acclimatized to the animal house for 1 week. All mice were housed in groups
117 of four and maintained in environmentally controlled conditions (temperature 22-
118 24ºC, 12h dark-light cycles and 51-53% relative humidity).
119 Animals received food and water *ad libitum* and were monitored daily for
120 health status. Body weight and food intake were recorded weekly. After
121 acclimatization, mice were randomly allocated into 3 groups (n=8 mice per group) to
122 receive either a standard chow diet (CD, A04, Scientific Animal Food & Engineering,
123 Augy, France), a high-fat diet (HFD, D12492, Ssniff Speziäten GmbH, Ferdinand-Gabriel-
124 Weg, Germany), or a high fat high-sucrose diet (HF-HSD, TD08811, Harlan Laboratories
125 Inc., Madison, WI, USA) for 20 weeks. Diet compositions are shown in Supplementary
126 Table 1. At the end of the experiment, mice were sacrificed following a12h fast. The
127 liver, adipose tissue and sera were collected and stored at -80ºC for biochemical and
128 molecular analyses, or preserved in formalin for histopathological analysis.

129 *2.2. Standard biochemical analyses*

130 Serum concentrations of glucose, cholesterol and triglycerides were
131 determined by standard tests in a Cobas Mira automated analyzer (Roche Diagnostics,
132 Rotkreuz, Switzerland).

133 *2.3. Histological analysis*

134 Liver and adipose tissue samples were fixed in formalin and embedded in
135 paraffin for hematoxylin and eosin staining. The degree of hepatic impairment was
136 estimated using the NAFLD activity score (NAS score). This scoring system is based on

137 histological features classified into three categories: steatosis (graded from 0 to 3),
138 lobular inflammation (graded from 0 to 2) and hepatocellular ballooning (graded from
139 0 to 2) were assessed by an experienced pathologist [18]. Samples were considered to
140 have NASH when the NAS score was ≥5. The average adipocyte size from visceral and
141 subcutaneous adipose tissue was estimated using the ImageJ 1.51 software (National
142 Institutes of Health, Bethesda, MD, USA) with the macro MRI's adipocyte tool.

143 *2.4. Immunohistochemistry*

144 To assess differences in oxidation and inflammation between the groups of
145 mice, we analyzed the hepatic immunohistochemical expressions of 4-hydroxy-2-
146 nonenal (marker of lipid peroxidation), paraoxonase-1 (an antioxidant enzyme),
147 chemokine (C-C motif) ligand-2 (CCL2), tumor necrosis factor-α (TNF-α), F4/80 antigen
148 (marker of total number of macrophages, both pro- and anti-inflammatory), cluster
149 differentiation 11b (CD11b, marker of pro-inflammatory macrophages), cluster
150 differentiation 163 (CD163, marker of anti-inflammatory macrophages), and C-type
151 lectin domain (CLEC4F, marker of Kupffer cells and infiltrating monocytes) [19,20]. The
152 employed primary antibodies are described in Supplementary Table 2. Unstained
153 paraffin-embedded tissues were deparaffinized and rehydrated before antigen
154 retrieval detection with 10 mM of sodium citrate or Tris-EDTA (10mM Tris Base, 1mM
155 EDTA) at pH 9.0 for 40 min at 95ºC. Endogenous peroxidase activity was blocked using
156 EnVison™ FLEX Peroxidase-Blocking Reagent (Agilent Technologies, Santa Clara, CA,
157 USA) for 25 minutes, and BSA 2% (Sigma Aldrich, St. Louis, MO, USA) was used to block
158 non-specific binding sites. Sections were incubated overnight with the corresponding
159 primary antibody, washed (twice for 4 min) with phosphate-buffered saline with
160 glycine, and incubated with EnVison™ FLEX/HRP (Agilent Technologies) for 1h at room
161 temperature. In the final step, slides were washed with phosphate-buffered saline with
162 glycine (twice for 4 min) and incubated with EnVison™ FLEX DAB + Chromogen (Agilent
163 Technologies). Photographs were taken with an optical microscope (Eclipse E600,
164 Nikon, Tokyo, Japan) and NIS-Elements F 4.00.00 software. Positively-stained areas
165 were calculated using the ImageJ 1.51 software (National Institutes of Health,
166 Bethesda, MD, USA) with the plug-in versatile wand tool.

167

168 *2.5. Plasma antioxidant capacity assay*

169 Plasma antioxidant capacity was measured by the ferric ion reducing
170 antioxidant power (FRAP) assay, as described previously [21] and performed using a
171 Biotek Power Wave XS microplate reader equipped with Gen5 software (Biotek
172 Instruments, Winooski, VT, USA). Trolox was used as a standard. Results were
173 expressed as mmol of Trolox Equivalents per liter (TE/L)

174 *2.6. Hepatic antioxidant enzyme assays*

175 Liver tissues (150 mg) were homogenized with a Politron (Thomas Scientific,
176 Swedesboro, NJ, USA) in 0.2M cold sodium phosphate buffer at pH 6.25. The crude
177 soluble fraction was obtained by ultra-centrifugation at 105,000 x g for 60 min at 4°C
178 (Kontron 50TI rotor and Centrikon T-1045 centrifuge, Kontron Instruments, Augsburg,
179 Germany). The supernatants were dispensed into aliquots to determine the different
180 enzymes. Protein content was measured with the Bradford method [22] using bovine
181 serum albumin as standard. Total superoxide dismutase (SOD) and catalase (CAT)
182 activities were measured as previously described [23,24]; results are presented as U/g
183 tissue and mmol/g tissue, respectively. Glutathione reductase (GR) and glutathione
184 peroxidase (GPX) activities were measured in a Cobas Mira automated analyzer
185 (Roche) [25]; the results are presented as U/g tissue.

186 *2.7. Targeted metabolomics*

187 We analyzed the hepatic concentrations of metabolites from glycolysis,
188 pentose-phosphate pathway, citric acid cycle (CAC), and amino acids as described in
189 detail previously [26]. Briefly, samples were injected into a 7890A gas chromatograph
190 coupled with an electron impact source to a 7200-quadrupole time-of-flight mass
191 spectrometer equipped with a 7693 auto-sampler module and a J&W Scientific HP-
192 5MS column (30 m × 0.25 mm, 0.25 µm; Agilent Technologies).

193 *2.8. Targeted lipidomics*

194 Adipose tissues (10 mg) were homogenized in a Precellys 24 homogenizer
195 (Bertin Technologies, Montigny, France) and polar lipids were extracted by adding 250
196 µL of methanol containing the selected internal standards described in Supplementary

197 Table 3. Samples were centrifuged at 15,000 rpm for 10 min at 4 ºC. The supernatants
198 were dispensed into glass vials for liquid chromatography and mass spectrometry (LC-
199 MS) analysis. Stock standards for calibration curves were dissolved in methanol at the
200 concentrations described in Supplementary Table 4. A series of 10 concentrations of
201 the internal standards mixture was prepared and dispensed into glass vials for LC-MS
202 analysis. Samples (5 µl) were injected into a 1290 Infinity ultra-high-pressure liquid
203 chromatograph (UHPLC) coupled to a 6550 quadrupole-time-of-flight mass
204 spectrometer (QTOF) using a dual jet stream electrospray ionization (ESI) source
205 (Agilent Technologies). The samples were injected in duplicate into the LC-MS system
206 working in positive and negative mode. Supplementary Table 5 describes the retention
207 times, *m/z* and polarity (positive or negative) in detecting each lipid species, as well as
208 the standards employed. The UHPLC system was equipped with a binary pump
209 (G4220A), an autosampler (G4226A) thermostat-controlled at 4ºC, and an Acquity BEH
210 C_{18} column 1.7 µm, 2.1 mm × 100 mm (Waters Corp., Milford, MA, USA) thermostat-
211 controlled at 40 ºC. The mobile phase consisted of A: water + 0.05% formic acid; B:
212 acetonitrile + 0.05 formic acid. The flow rate was 0.3 mL/min. The gradient used was as
213 follows: 0 min, 2% B; 2 min, 50% B; 10 min, 98% B; from 10 to 13 min, gradient was
214 maintained at 98% B for column cleaning; 14 min, 2% B followed by a post-run of 4
215 min under the same conditions for column re-conditioning. For the ESI source, the
216 optimized parameters were as follows: gas temperature 225 ºC, drying gas flow 11
217 L/min, nebulizer 35 psi, sheath gas temperature 300 ºC and sheath gas flow 12 L/min
218 For the QTOF-MS, the capillary, nozzle and fragmentor voltages were set at 3500 V,
219 500 V and 380 V, respectively.

220 *2.9. GC-MS and LC-MS metabolites quantification*

221 Metabolites and lipid species were quantified using Mass Hunter Quantitative
222 Analysis B.07.00 (Agilent Technologies). Lipid characterization was done by matching
223 their accurate mass and isotopic distributions to the Metlin-PCDL database (Agilent
224 Technologies) allowing a mass error of 10 ppm and a score higher than 80 for isotopic
225 distribution. To ensure the tentative characterization, chromatographic behavior of
226 pure standards and corroboration with Lipid Maps database (www.lipidmaps.org) was
227 performed.

228 *2.10. Immunoblotting analysis*

229 Frozen hepatic tissues (30 mg) were homogenized with 300 µL of 0.25M
230 sucrose. Adipose tissues (100 mg) were homogenized with 200 µl RIPA (Sigma Aldrich)
231 in a 2mL safe-lock Eppendorf tube. Both buffers contained phosphatase (Roche
232 Diagnostics) and protease inhibitors (Roche Diagnostics). After centrifugation (14,000
233 rpm, 4ºC, 20 min) the protein concentration was analyzed in the aqueous phase using
234 a NanoDrop2000 spectrophotometer (Thermo Fisher Scientific Inc. Waltham, MA,
235 USA). We analyzed the hepatic expressions of AMP-activated protein kinase (AMPK)
236 and acetyl-CoA carboxylase (ACC) and their inactive phosphorylated forms pAMPK and
237 pACC, hormone sensitive lipase (HSL) and pHSL**,** mammalian target of rapamycin
238 complex 1 (mTORC1) and pmTORC1, autophagy-related protein 7 (ATG7),
239 microtubule-associated proteins 1A/1B light chain 3B (LC3B), mitofusin 2 (MFN2),
240 total oxidative phosphorylation (OXPHOS), CCL2, CD11b, CD163, c-Jun and p-c-Jun,
241 sequestosome-1 (P62) and pP62, PTEN-induced putative kinase 1 (PINK1), E3 ubiquitin-
242 protein ligase parkin (PARKIN), translocase outer membrane 20 (TOM20), fatty acid
243 synthase (FASN) and uncoupling protein 1 (UCP-1). Denatured proteins (50 µg) from
244 frozen tissue were subjected to 8%–14% sodium dodecyl sulfate polyacrylamide gel or
245 nitrocellulose membrane electrophoresis with a Trans-Blot Turbo Transfer System (Bio-
246 Rad Laboratories, Hercules, CA, USA). Membranes were incubated for 1h in a blocking
247 solution (5% non-fat dry milk in Tris-buffered saline with 0.1% Tween-20). Samples
248 were, then, incubated with the corresponding primary antibody as described in
249 Supplementary Table 2. The following day, membranes were washed (thrice for 10
250 min) in Tris-buffered saline and incubated for 1h at room temperature in the presence
251 of polyclonal goat anti-rabbit (HRP) antibody (Agilent Technologies). Membranes were
252 washed again (thrice for 10 min) in Tris-buffered saline and enhanced with SuperSignal
253 West Femto chemiluminescent substrate (ThermoFisher) and image were digitally
254 captured using de ChemiDoc MP System (Bio-Rad). Bands were quantified using Image
255 Lab software (Bio-Rad) and the protein expressions were normalized with a
256 housekeeping protein (FAH).

257

258

259 *2.11. Extraction and quantification of RNA*

260 Total RNA was extracted from liver using RNeasy kit (Qiagen, Barcelona, Spain)
261 according to the manufacturer's instructions, and was purified by chloroform
262 extraction and isopropanol precipitation. RNA concentration and purity were
263 determined using Nanodrop ND-2000 spectrophotometer (Thermofisher Scientific).
264 Quantitative gene expression was evaluated by qPCR on a 7900HT Fast Real-Time PCR
265 System using TaqMan Gene Expression Assay (Applied Biosystems) with the primer
266 sequences ATP-citrate lyase (Mm01302282_m1), isocitrate dehydrogenase 1
267 (Mm00516030_m1), isocitrate dehydrogenase 2 (Mm00612429_m1), oxoglutarate
268 dehydrogenase (Mm00803119_m1) and succinate dehydrogenase
269 (Mm01352366_m1). Beta-2-microglobulin (B2M) was employed as housekeeping
270 gene.

271 *2.12. Statistical analysis*

272 Data are presented as mean ± standard error of the mean (SEM) unless
273 otherwise indicated. Differences between groups were analyzed by the Mann-Whitney
274 *U*-test with the SPSS package, version 22.0. MetaboAnalyst 4.0 (available at
275 http://www.metaboanalyst.ca/) was used to generate scores/loading plots and
276 Heatmaps. Multivariate statistics were used to improve the analysis of complex raw
277 data and pattern recognition. The supervised partial least squares discriminant analysis
278 (PLSDA) method was employed to distinguish the compared groups according to
279 metabolomic data. The relative magnitude of observed changes was evaluated using
280 the variable importance in projection (VIP) score. Statistical significance was defined
281 when p value was <0.05.

282 **3. Results**

283 *3.1. HFD and HF-HSD promoted NAFLD, but only HF-HSD promoted NASH*

284 Mice fed HFD and HF-HSD showed a faster gain in body weight than the CD-fed
285 group (Fig. 1A). The relative food intake was higher in the CD-fed group due to the
286 lower energy density of this diet, but there were no differences in calorie intake
287 between groups (Fig. 1B and C). At sacrifice, animals fed HFD and HF-HSD showed
288 significantly higher serum cholesterol concentrations than CD-fed animals, but only

289 mice fed HF-HSD showed significantly increased circulating glucose and triglycerides
290 (Fig. 1D). Hepatic histology was normal in CD-fed mice. In contrast, animals fed HFD
291 showed a general loss of hepatocyte structure, and with an increase in cytosolic fat
292 accumulation characteristic of NAFLD. In mice fed HFD, fat accumulation was observed
293 predominantly as micro-vesicular steatosis with some ballooning. Histopathological
294 alterations were more severe in mice fed HF-HSD. This group, apart from presenting
295 micro-vesicular steatosis in the peri-central area, had macro-vesicular steatosis in the
296 peri-portal area, severe ballooning, and lobular inflammation (Fig. 1F). In mice fed HFD
297 and HF-HSD, changes in liver histology were accompanied with a significant increase of
298 liver weight compared to CD-fed animals. Only mice fed HF-HSD showed NAS scores
299 >5: indicating the presence of NASH.

300 *3.2. HF-HSD was associated with oxidative stress and inflammation*

301 In mice fed HF-HSD, we found a significantly increased hepatic
302 immunohistochemical expression of 4-hydroxy-2-nonenal, which is the most abundant
303 product derived from peroxidation of polyunsaturated fatty acids. The expression of
304 the antioxidant enzyme PON1 remained unmodified (Fig. 2A). This increase in lipid
305 peroxidation was accompanied by lower hepatic SOD, CAT and GPX activities, while
306 there were no significant changes in GR. In addition, these mice showed a significant
307 decrease in plasma FRAP (Fig. 2B). Moreover, the oxidative stress environment was
308 corroborated with the activation of c-Jun (Ser 73), which is a major redox-sensitive
309 component (Fig. 2C).This general increase in oxidative stress may stimulate
310 inflammatory response. To investigate this issue, we focused on markers present in
311 macrophages that are key players in initiating an immune response. Our results
312 showed that mice fed HFD and HF-HSD had a lower expression of CLEC4F and F4/80
313 than CD-fed animals (Supplementary Fig.1A). In addition, CD163 expression was also
314 lower; indicating a poor anti-inflammatory response in mice fed HF-HSD and HFD. The
315 lower anti-inflammatory capacity was accompanied by the increase of pro-
316 inflammatory marker CD11b in both groups, although the increase was stronger in the
317 HF-HSD group. Moreover, expression of the inflammatory chemokine (C-C motif)
318 ligand-2 (CCL2) was significantly increased in mice fed HF-HSD (Supplementary Fig. 1B).

319 *3.3. HF-HSD was associated with metabolic inflexibility in adapting to excess nutrient*
320 *intake*

321 PLDSA analysis showed significant global liver differences in energy balance-
322 related metabolites between the different diets administered. VIP analysis showed
323 that the variations in the metabolite profile were attributed mainly to oxaloacetate,
324 fructose-6-P, fructose-1,6-BisP, glucose-6-P, α-ketoglutarate, 6-P-gluconate, citrate,
325 and ribose-5-P, all of which had VIP values >1 (Supplementary Fig. 2). HFD and HF-HSD
326 produced different alterations in metabolites of the CAC cycle, glycolysis, amino acids
327 and pentose-phosphate pathway (PPP) (Table 1, Supplementary Fig. 3). HFD-fed mice
328 had significant increases of some metabolites involved in pathways of glycolysis and
329 PPP, whereas animals fed HF-HSD had lower levels of these metabolites than CD-fed
330 mice. Immunoblotting analyses (Fig. 3A) suggested that mice fed HF-HSD had a poorer
331 metabolic adaptation (metabolic inflexibility) due to a relative incapacity to oxidize the
332 accumulated lipids and to an increase the lipogenic pathways via the upregulation of
333 ACC1 and FASN. In contrast to mice fed HF-HSD, animals fed HFD showed an adequate
334 metabolic adaptation by increasing the mitochondrial fatty acid oxidation via the
335 inhibition of ACC2, and downregulation of key proteins in pathways of lipogenesis. We
336 also investigated whether this switch in liver metabolism was related to alterations in
337 mitochondrial proteins. We found low levels of mitochondrial complexes II, III and V,
338 suggesting a decrease in the capacity to oxidize succinate to fumarate and to produce
339 ATP. Finally, we analyzed the gene expression of ATP-citrate lyase (ACLY), isocitrate
340 dehydrogenase 1 and 2 (IDH1 and 2), oxoglutarate dehydrogenase (OGHD) and
341 succinate dehydrogenase (SDHA) (Fig. 3B). The mice fed HF-HSD showed a great
342 increase expression of ACLY and IDH1 and a moderate increase of SDHA and OGDHA,
343 suggesting a rewriting metabolic flux towards lipogenesis. As such, these results
344 suggest that the increase in hepatic *de novo* lipogenesis (DNL) in mice fed HF-HSD
345 might be a compensatory response to the lowered capacity for oxidative metabolism
346 in the mitochondria.

347

348

349 *3.4. HF-HSD promoted defective mitochondrial clearance via autophagy*

350 We evaluated whether autophagy was inhibited within the context of
351 metabolic inflexibility. As shown in Fig. 4, the activation of AMP-activated protein
352 kinase (AMPK) suggested the activation of autophagy , with the formation of auto-
353 phagosomes and the increase in LC3II in the HF-HSD group. However, the increase in
354 P62 levels suggests a blockage in the final step of the pathway resulting in the
355 accumulation of non-degraded auto-phagosomes. We further assessed whether the
356 inhibition of autophagy was associated with the inhibition of ubiquitin-dependent
357 mitophagy. For this purpose, we determined the levels of pP62, PINK and PARKIN that
358 are necessary for normal mitophagy function. As shown in Fig. 4, we observed high
359 levels of all three proteins, indicating a high number of malfunctioning mitochondria
360 and accumulation of proteins awaiting degradation. Finally, we investigated the
361 capacity of the mitochondria to incorporate new mitochondrial pre-proteins through
362 the TOM20 pathway. We observed that the levels of this protein were lower;
363 indicating, again, a metabolic blockage of the mitochondria. All these results indicate a
364 poorer metabolic adaptation in animals fed HF-HSD.

365 *3.5. Diet induces metabolic re-programming of adipose tissue*

366 The results obtained so far indicate that liver metabolism was strongly altered
367 in the mice fed HF-HSD. But we were curious to know whether different diets change
368 the adipose tissue dynamics. As shown in Fig. 5A-C, the adipocyte size increased
369 (hypertrophy) in the peri-gonadal WAT (pgWAT) and the inguinal WAT (iWAT) of the
370 groups fed HFD and HF-HSD. Following this observation, we studied the role of several
371 proteins involved in processes related to lipogenesis and to lipolysis. We observed a
372 downregulation of ACC1 and HSL, resulting in a lower capacity to store (lipogenesis)
373 and to remove (lipolysis) excess triglycerides, and lower thermogenic capacity by UCP-
374 1 (Fig 5D).

375 *3.6. HF-HSD is associated with the accumulation of visceral lipid species*

376 We proceeded to measure the concentrations of a wide range of lipid species in
377 the liver, pgWAT and iWAT. Results of the individual lipids measured are summarized
378 in Supplementary Tables 6, 7 and 8. Globally, lipid content differed according to the

379 diet administered, and to the anatomical location of the tissue in which the
380 measurements were made. There was a significant accumulation of saturated fatty
381 acids (SFA) and polyunsaturated fatty acids (PUFA) in pgWAT as well as iWAT of the
382 mice fed HF-HSD; while the HFD-group showed a decrease in SFA in iWAT, and no
383 changes in pgWAT in the animals fed CD (Supplementary Fig. 4). In contrast, the
384 content of PUFA was decreased in iWAT of mice fed HFD and HF-HSD, while PUFA
385 content in pgWAT was only decreased in the HFD-group. In addition, there were
386 variations in the concentrations of bile acid metabolites; a decrease in cholic acid (CA)
387 metabolites only in iWAT of the HF-HSD-group; suggesting an impairment in energy
388 expenditure [27]. These results suggest that the impairment of iWAT function in mice
389 fed HF-HSD completely abolished the capacity of the animal to store excess circulating
390 free fatty acids, while promoting lipid accumulation in pgWAT (Fig. 6).

391 **4. Discussion**

392 Results of the present study show that, in mice receiving a high-fat diet, the
393 addition of sucrose promotes the development of NASH. In this context, sucrose acts
394 as a lesion enhancer by inducing the inhibition of autophagy and fatty acid oxidation
395 and, concomitantly, activating *de novo* lipogenesis. Also, the sucrose induces adipose
396 tissue dynamic changes. Both HFD and HF-HSD diets were obesogenic but the effects
397 produced at the metabolic and mechanistic level were different. Previous studies
398 evidenced the lack of consensus on the most effective diets (and duration of exposure
399 to them) to induce metabolic alterations and related pathologies such as diabetes,
400 metabolic syndrome, NAFLD or NASH [28]. In rats, the feeding of HFD or HF-HSD
401 caused steatosis, but not NASH [29,30], while diets with a very high sucrose content
402 (without excess fat), were able to promote steatosis and NASH [31,32]. In contrast, a
403 diet high in sucrose and fat does induce steatosis [33] as well as NASH [34,35] in mice.
404 Earlier reports [36,37] indicated that different diets act as modulators of different
405 alterations in metabolism, depending on the nutritional composition of the diets. A
406 more recent report [38] showed that fructose supplementation in HFD alters the
407 mitochondrial protein acetylation involved in hepatic fatty acid oxidation (FAO).

408 We have corroborated these observations in a long-term study showing that
409 the administration of a HF-HSD to mice, not only induces metabolic changes in liver

410 but also in different regions of adipose tissue. These findings correlated with the
411 aggravation of NAFLD and the appearance of NASH. We also observed that sucrose
412 supplementation in HFD promoted oxidative stress and activation of the immune
413 response i.e. the immune cells developed an imbalance of pro-inflammatory/anti-
414 inflammatory markers in favor of an increase in pro-inflammatory CD11b expression.
415 This observation is supported by other reports showing that the administration of
416 high-fat, high-cholesterol, high-sugar diet [39] or high-fat high-cholesterol diet [40] in
417 mice promoted an increase of CD11b levels and the number of M1 macrophages. In
418 addition, the upregulation of inflammatory response was associated with an increase
419 in oxidative stress through the inhibition of hepatic SOD, CAT and GPx activity and the
420 activation of c-Jun. One report indicated that obese patients with NASH had a lower
421 antioxidant defense capacity [41], which was in line with another report in a murine
422 NASH model [42]. Further, this obesogenic phenotype was linked to changes in
423 metabolic regulation. Strikingly, the activation of AMPK and mTORC1 was different
424 depending on the diet. In the present study, the administration of HF-HSD stimulated
425 AMPK without effecting autophagy activation, since the process was blocked at the
426 last step of lysosome fusion. With regard to this observation, it is of note that the
427 activation of AMPK is known to induce autophagy in general while, in contrast,
428 mTORC1 promotes the inhibition of autophagosome formation [43]. For example, mice
429 deficient in carboxylesterase 1d (Ces1d) are protected from NAFLD induction by HF-
430 HSD *via* activation of AMPK [44]. However, other factors such as the exposure to
431 certain lipid species, the activation of Rubicon (a negative regulator of autophagy), or
432 the preference of autophagosomes to fuse with endosomes (low hydrolysis efficiency)
433 may regulate the autophagosome-lysosome fusion step [45–47]. This could explain the
434 increase of LC3-II and P62 observed in HF-HSD. We noted that HFD administration
435 produced a decrease of LC3-II and P62 levels, reflecting a normal autophagic flux;
436 albeit this was associated with the surprising activation of mTORC1. One explanation
437 of this autophagy flux could be the activation of p38-mitogen-activated protein kinase
438 (p38 MAPK) that, under certain stress stimuli, may induce autophagy activation, thus
439 acting as a compensatory measure to restore homoeostasis [48,49]. In this context, we
440 found that HFD is associated with the activation of p38 MAPK, implying that this factor
441 might be a countermeasure to defend liver tissue from injury. Of note is that HF-HSD

442 promoted the activation of PINK1/PARKIN pathway and the increase in MFN2 and p-
443 P62 levels; suggesting an activation of the mitophagy machinery as consequence of
444 abnormal mitochondrial accumulation. It is of further note that, despite the role
445 assigned to PINK1/PARKIN pathway in the clearance of abnormal mitochondria
446 (mitophagy), the results demonstrated a low capacity of the lysosome to degrade
447 autophagosomes, thus precluding the elimination of damaged mitochondria. In
448 concordance with our findings, a previous report highlighted that the increase of
449 MFN2 and PINK1/PARKIN pathway was linked to clearance of abnormal mitochondria
450 in cardiomyocytes. The authors suggested that PINK1 phosphorylates MFN2 to attract,
451 and bind, PARKIN to promote the ubiquitination of mitochondrial proteins [50]. In this
452 context, other reports observed that the genetic ablation of MFN2 in liver, or in
453 specific neurons, causes mitochondrial dysfunction and alterations in morphology
454 [51,52]. Further, a recent report showed that PINK/PARKIN pathway controls the
455 specific degradation of MFN 1 and 2 rather than the global mitochondrial
456 ubiquitination; thus indicating pathways other than ubiquitin may label damaged
457 mitochondria [53]. However, the implication of diet in the mitochondrial state seems
458 to be more complex than expected due to a contradictory results from a few studies.
459 These discrepancies can be due to a qualitative and quantitative variations of dietary
460 composition that influence the transition of NAFL to NASH [54].

461 We also observed that the activation of AMPK/mTORC1 promoted the
462 activation of ACC1 in mice fed HF-HSD, and the inhibition of ACC2 in mice fed HFD:
463 processes related to hepatic DNL and FAO respectively. Indeed, an explanation for this
464 switch in ACC1/ACC2 activation might be the presence, or absence, of fructose in the
465 diet; reports have suggested that fructose consumption enhances fatty acid synthesis
466 [55,56]. However, a recent study indicates that this response might depend on the
467 mouse strain: thus emphasizing the importance of the genetic background in
468 experimental-animal studies [57]. Of note is that supplementation of HFD with
469 sucrose promoted a different metabolic response to that of HFD alone. The exposure
470 to HF-HSD caused a decrease in the concentrations of metabolites of glycolysis, while
471 HFD caused an increase. The high numbers of damaged mitochondria and insulin
472 resistance may block glucose oxidation via CAC in favor of induction of reductive

473 carboxylation which supports the biosynthesis of lipids [58,59]. Finally, we observed
474 that adipose tissue may be crucial in aggravating NAFLD, and its progression to NASH.
475 Indeed, administering HFD or HF-HSD was sufficient to induce pgWAT and iWAT
476 hypertrophy. We also observed that both diets induced a metabolic re-programing of
477 adipose tissue, independently of the anatomical localization. As such, these diets
478 produced an increase in phosphorylated AMPK levels that led to the inhibition of
479 lipolysis, accompanied by a downregulation of ACC1; a process related to DNL. Some
480 evidence indicated that the downregulation of DNL appears to be a mechanism
481 responsible for insulin resistance in adipose tissue [60-62]. However, adipose tissue is
482 the largest organ and its metabolic function not only differs between anatomical
483 regions but also within regions, implying a complex regulation network. Of
484 considerable note is that there was an increase in the levels of SFA, MUFA and PUFA in
485 iWAT and, more importantly, in pgWAT of mice fed HF-HSD. Our results are in
486 agreement with a report showing that VAT contained more MUFA than SAT as a result
487 of a higher activity of long-chain fatty acid elongase 6 and steaoryl-CoA desaturase-1;
488 two enzymes involved in the elongation and desaturation of fatty acids[63]. This
489 observation can be explained by a decreased ability of subcutaneous adipose tissue to
490 expand contributing to deposition into visceral adipose tissue and the liver. Several
491 reports suggest that the reduction of visceral adipose tissue concomitantly reduces
492 insulin resistance and glucose levels in humans, and increases lifespan in animal
493 models [64–66]. In contrast, the reduction of subcutaneous adipose tissue has been
494 reported not to improve insulin sensitivity, and the subcutaneous increase in adipose
495 tissue is considered complicit in the metabolic complications related to obesity [67,68].
496 Our current findings highlight the interconnection between these organs and their
497 involvement in metabolic disease progression.

498 The mechanisms by which HF-HSD induces NAFLD and NASH are complex.
499 Indeed, and regardless of the results obtained in our study, reports have shown that
500 HF-HSD impairs phosphorylation of protein kinase B (PKB/Akt), hyperphosphorylation
501 of insulin receptor substrate-1, activation of poly (ADP-ribose) polymerase 1 (PARP-1),
502 altered mitochondrial function, and autophagy in experimental models. Conversely,
503 the administration of several nutraceuticals corrected these alterations while

activating anti-oxidative signaling pathways, reducing inflammation and modifying gut microbiota [69–75]. The combined results of studies published to-date highlight the close relationship between oxidative stress, mitochondrial dysfunction, alterations in autophagy and excessive accumulation of lipids in the development of NASH induced by HF-HSD.

This study has potential translational implications to human pathology. Our results point towards adipose tissue dysfunction as an important contributor to the progression of NAFLD to NASH and, as such, highlight the potential of adipose tissue as a therapeutic target for the management of metabolic complications of obesity. The results also highlight the importance of understanding the impact of two dietary patterns which, in our present case, were sufficient to induce two different phenotypes. We conclude that the administration of a HF-HSD under metabolic blockage conditions led to an oxidative and inflammatory environment, and negated the restoration of damaged hepatic mitochondria. In addition, the continuous accumulation of fatty acids resulted in dysfunctional adipose tissue, and hepatic fat accumulation that favored the progression to NASH. A limitation of the present study is that modifications in the autophagy process have been studied indirectly, by analyzing the expression of some regulatory factors. Dynamic studies, measuring autophagy flux activity would be necessary to fully demonstrate this hypothesis.

Funding

This study was supported by grants PI15/00285 and PI18/00921 from the *Instituto de Salud Carlos III* (Madrid, Spain); co-funded by European Social Fund (ESF); “Investing in your future” and the *Agència de Gestió d’Ajuts Universitaris i de Recerca* (SGR00436).

Author contributions

Gerard Baiges-Gaya, Jordi Camps, Jorge Joven: Conceptualization; Gerard Baiges-Gaya, Jordi Camps: Data curation; Gerard Baiges-Gaya, Jordi Camps, Jorge Joven: Formal analysis; Marta Romeu, Maria-Rosa Nogués, Jorge Joven: Funding acquisition; Gerard Baiges-Gaya, Salvador Fernández-Arroyo, Fedra Luciano-Mateo,

Noemí Cabré, Elisabet Rodríguez-Tomàs, Anna Hernández-Aguilera, Helena Castañé: Investigation; Gerard Baiges-Gaya, Salvador Fernández-Arroyo, Fedra Luciano-Mateo, Noemí Cabré, Elisabet Rodríguez-Tomàs, Anna Hernández-Aguilera, Helena Castañé: Methodology; Jordi Camps, Jorge Joven: Project administration; Salvador Fernández-Arroyo, Marta Romeu, Maria-Rosa Nogués, Jorge Joven: Resources; Gerard Baiges-Gaya, Salvador Fernández-Arroyo: Software; Jordi Camps, Jorge Joven: Supervision; Gerard Baiges-Gaya, Jordi Camps, Jorge Joven: Validation; Jordi Camps: Visualization; Gerard Baiges-Gaya: Writing – original draft; Jordi Camps: Writing – review & editing.

Declaration of competing interest

None.

545 **REFERENCES**

546 [1] González-Muniesa P, Mártinez-González M-A, Hu FB, Després J-P, Matsuzawa Y, F Loos
547 RJ, et al. Obesity, considered by many as a 21st century epidemic. Nat Publ Gr
548 2017;3:1–18. https://doi.org/10.1038/nrdp.2017.34.

549 [2] Friedman SL, Neuschwander-Tetri BA, Rinella M, Sanyal AJ. Mechanisms of NAFLD
550 development and therapeutic strategies. Nat Med 2018;24:908–22.
551 https://doi.org/10.1038/s41591-018-0104-9.

552 [3] Van Dam RM, Seidell JC. Carbohydrate intake and obesity. Eur J Clin Nutr 2007. 61 suppl
553 1;s75–99. https://doi.org/10.1038/sj.ejcn.1602939.

554 [4] Stanhope KL. Sugar consumption, metabolic disease and obesity: The state of the
555 controversy. Crit Rev Clin Lab Sci 2016;53:52–67
556 https://doi.org/10.3109/10408363.2015.1084990.

557 [5] Schuster S, Cabrera D, Arrese M, Feldstein AE. Triggering and resolution of
558 inflammation in NASH. Nat Rev Gastroenterol Hepatol 2018;15:349–64.
559 https://doi.org/10.1038/s41575-018-0009-6.

560 [6] Kim D, Kim W, Joo SK, Han J, Kim JH, Harrison SA, et al. Association between body size-
561 metabolic phenotype and nonalcoholic steatohepatitis and significant fibrosis. J
562 Gastroenterol 2019. https://doi.org/10.1007/s00535-019-01628-z.

563 [7] Hoffstedt J, Arner E, Wahrenberg H, Andersson DP, Qvisth V, Löfgren P, et al. Regional
564 impact of adipose tissue morphology on the metabolic profile in morbid obesity.
565 Diabetologia 2010;53:2496–503. https://doi.org/10.1007/s00125-010-1889-3.

566 [8] Tchkonia T, Thomou T, Zhu Y, Karagiannides I, Pothoulakis C, Jensen MD, et al.
567 Mechanisms and metabolic implications of regional differences among fat depots. Cell
568 Metab 2013;17:644–56. https://doi.org/10.1016/j.cmet.2013.03.008.

569 [9] White UA, Tchoukalova YD. Sex dimorphism and depot differences in adipose tissue
570 function. Biochim Biophys Acta-Mol Basis Dis 2014;1842:377–92.
571 https://doi.org/10.1016/j.bbadis.2013.05.006.

572 [10] Arner P, Bernard S, Salehpour M, Possnert G, Liebl J, Steier P, et al. Dynamics of human
573 adipose lipid turnover in health and metabolic disease. Nature 2011;478:110–3.
574 https://doi.org/10.1038/nature10426.

575 [11] Tchoukalova YD, Votruba SB, Tchkonia T, Giorgadze N, Kirkland JL, Jensen MD. Regional
576 differences in cellular mechanisms of adipose tissue gain with overfeeding. Proc Natl
577 Acad Sci U S A 2010;107:18226–31. https://doi.org/10.1073/pnas.1005259107.

578 [12] Frayn, K. Adipose tissue as a buffer for daily lipid flux. *Diabetologia* **45,** 1201–1210
579 (2002). https://doi.org/10.1007/s00125-002-0873-y

580 [13] Virtue S, Petkevicius K, Moreno-Navarrete JM, Jenkins B, Hart D, Dale M, et al.
581 Peroxisome Proliferator- Activated Receptor γ2 Controls the Rate of Adipose Tissue
582 Lipid Storage and Determines Metabolic Flexibility. Cell Rep. 2018;24(8):2005-2012.e7.
583 doi:10.1016/j.celrep.2018.07.063[14] Asterholm IW, Mundy DI, Weng J, Anderson
584

585 [14] RG, Scherer PE. Altered mitochondrial function and metabolic inflexibility associated
586 with loss of caveolin-1. Cell Metab. 2012;15(2):171-185.
587 doi:10.1016/j.cmet.2012.01.004
588

589 [15] Mendez-Sanchez N, Cruz-Ramon VC, Ramirez-Perez OL, Hwang JP, Barranco-Fragoso B,
590 Cordova-Gallardo J. New aspects of lipotoxicity in nonalcoholic steatohepatitis. Int J
591 Mol Sci 2018;19: pii: E2034. https://doi.org/10.3390/ijms19072034.

592 [16] Lim JS, Mietus-Snyder M, Valente A, Schwarz JM, Lustig RH. The role of fructose in the
593 pathogenesis of NAFLD and the metabolic syndrome. Nat Rev Gastroenterol Hepatol
594 2010;7:251–64. https://doi.org/10.1038/nrgastro.2010.41.

595 [17] Yamada T, Murata D, Adachi Y, Itoh K, Kameoka S, Igarashi A, et al. Mitochondrial stasis
596 reveals p62-mediated ubiquitination in parkin-independent mitophagy and mitigates
597 nonalcoholic fatty liver disease. Cell Metab 2018;28:588–604.
598 https://doi.org/10.1016/j.cmet.2018.06.014.

599 [18] Kleiner DE, Brunt EM, Van Natta M, Behling C, Contos MJ, Cummings OW, et al. Design
600 and validation of a histological scoring system for nonalcoholic fatty liver disease.
601 Hepatology 2005;15:1313–21. https://doi.org/10.1002/hep.20701.

602 [19] Luciano-Mateo F, Cabré N, Fernández-Arroyo S, Baiges-Gaya G, Hernández-Aguilera A,
603 Rodríguez-Tomàs E, et al. Chemokine (C-C motif) ligand 2 gene ablation protects low-
604 density lipoprotein and paraoxonase-1 double deficient mice from liver injury, oxidative
605 stress and inflammation. Biochim Biophys Acta - Mol Basis Dis 2019;1865:1555–1566.
606 https://doi.org/10.1016/j.bbadis.2019.03.006.

607 [20] Cabré N, Luciano-Mateo F, Fernández-Arroyo S, Baiges-Gayà G, Hernández-Aguilera A,
608 Fibla M, et al. Laparoscopic sleeve gastrectomy reverses non-alcoholic fatty liver
609 disease modulating oxidative stress and inflammation. Metabolism 2019;99:81–89.
610 https://doi.org/10.1016/j.metabol.2019.07.002.

611 [21] Benzie IFF, Strain JJ. The ferric reducing ability of plasma (FRAP) as a measure of
612 "antioxidant power": The FRAP assay. Anal Biochem 1996;239:70–6.
613 https://doi.org/10.1006/abio.1996.0292.

614 [22] Bradford MM. A rapid and sensitive method for the quantitation of microgram
615 quantities of protein utilizing the principle of protein-dye binding. Anal Biochem
616 1976;72:248–54. https://doi.org/10.1016/0003-2697(76)90527-3.

617 [23] Misra HP, Fridovich I. The role of superoxide anion in the autoxidation of epinephrine
618 and a simple assay for superoxide dismutase. J Biol Chem 1972;247:3170–5.

619 [24] Cohen G, Dembiec D, Marcus J. Measurement of catalase activity in tissue extracts. Anal
620 Biochem 1970;34:30–8. https://doi.org/10.1016/0003-2697(70)90083-7.

621 [25] Wheeler CR, Salzman JA, Elsayed NM, Omaye ST, Korte DW. Automated assays for
622 superoxide dismutase, catalase, glutathione peroxidase, and glutathione reductase
623 activity. Anal Biochem 1990;184:193–9. https://doi.org/10.1016/0003-2697(90)90668-
624 Y.

625 [26] Riera-Borrull M, Rodríguez-Gallego E, Hernández-Aguilera A, Luciano F, Ras R, Cuyàs E,
626 et al. Exploring the Process of Energy Generation in Pathophysiology by Targeted
627 Metabolomics: Performance of a Simple and Quantitative Method. J Am Soc Mass
628 Spectrom. 2016;27(1):168-177. https:// doi:10.1007/s13361-015-1262-3

629 [27] Watanabe M, Houten SM, Mataki C, Christoffolete MA, Kim BW, Sato H, et al. Bile acids
630 induce energy expenditure by promoting intracellular thyroid hormone activation.
631 Nature 2006;439:484–9. https://doi.org/10.1038/nature04330.

632 [28] Melo BF, Sacramento JF, Ribeiro MJ, Prego CS, Correia MC, Coelho JC, et al. Evaluating
633 the impact of different hypercaloric diets on weight gain, insulin resistance, glucose
634 intolerance, and its comorbidities in rats. Nutrients 2019;11: pii: E1197.
635 https://doi.org/10.3390/nu11061197.

636 [29] Roberts MD, Mobley CB, Toedebush RG, Heese AJ, Zhu C, Krieger AE, et al. Western
637 diet-induced hepatic steatosis and alterations in the liver transcriptome in adult Brown-

638 Norway rats. BMC Gastroenterol 2015;15:151. https://doi.org/10.1186/s12876-015-
639 0382-3.

640 [30] Fakhoury-Sayegh N, Trak-Smayra V, Khazzaka A, Esseily F, Obeid O, Lahoud-Zouein M,
641 et al. Characteristics of nonalcoholic fatty liver disease induced in wistar rats following
642 four different diets. Nutr Res Pract 2015;9:350–7.
643 https://doi.org/10.4162/nrp.2015.9.4.350.

644 [31] Ragab SMM, Abd Elghaffar SK, El-Metwally TH, Badr G, Mahmoud MH, Omar HM. Effect
645 of a high fat, high sucrose diet on the promotion of non-alcoholic fatty liver disease in
646 male rats: The ameliorative role of three natural compounds. Lipids Health Dis
647 2015;14:83. https://doi.org/10.1186/s12944-015-0087-1.

648 [32] Acosta-Cota S de J, Aguilar-Medina EM, Ramos-Payán R, Ruiz-Quiñónez AK, Romero-
649 Quintana JG, Montes-Avila J, et al. Histopathological and biochemical changes in the
650 development of nonalcoholic fatty liver disease induced by high-sucrose diet at
651 different times. Can J Physiol Pharmacol 2019;97:23–36. https://doi.org/10.1139/cjpp-
652 2018-0353.

653 [33] Wang S, Yang FJ, Shang LC, Zhang YH, Zhou Y, Shi XL. Puerarin protects against high-fat
654 high-sucrose diet-induced non-alcoholic fatty liver disease by modulating PARP-
655 1/PI3K/AKT signaling pathway and facilitating mitochondrial homeostasis. Phyther Res
656 2019;33:2347–2359. https://doi.org/10.1002/ptr.6417.

657 [34] Verbeek J, Lannoo M, Pirinen E, Ryu D, Spincemaille P, Elst I Vander, et al. Roux-en-y
658 gastric bypass attenuates hepatic mitochondrial dysfunction in mice with non-alcoholic
659 steatohepatitis. Gut 2015;64:673–83. https://doi.org/10.1136/gutjnl-2014-306748.

660 [35] Verbeek J, Spincemaille P, Vanhorebeek I, Van Den Berghe G, Vander Elst I,
661 Windmolders P, et al. Dietary intervention, but not losartan, completely reverses non-
662 alcoholic steatohepatitis in obese and insulin resistant mice. Lipids Health Dis
663 2017;16:46. https://doi.org/10.1186/s12944-017-0432-7.

664 [36] Drescher HK, Weiskirchen R, Fülöp A, Hopf C, De San Román EG, Huesgen PF, et al. The
665 influence of different fat sources on steatohepatitis and fibrosis development in the
666 western diet mouse model of non-alcoholic steatohepatitis (NASH). Front Physiol
667 2019;10:770. https://doi.org/10.3389/fphys.2019.00770.

668 [37] Softic S, Gupta MK, Wang GX, Fujisaka S, O'Neill BT, Rao TN, et al. Divergent effects of

669 glucose and fructose on hepatic lipogenesis and insulin signaling. J Clin Invest
670 2017;11:4059–4074. https://doi.org/10.1172/JCI94585.

671 [38] Softic S, Meyer JG, Wang GX, Gupta MK, Batista TM, Lauritzen HPMM, et al. Dietary
672 sugars alter hepatic fatty acid oxidation via transcriptional and post-translational
673 modifications of mitochondrial proteins. Cell Metab 2019;30:735–753.e4.
674 https://doi.org/10.1016/j.cmet.2019.09.003.

675 [39] Ambade A, Satishchandran A, Saha B, Gyongyosi B, Lowe P, Kodys K, et al.
676 Hepatocellular carcinoma is accelerated by NASH involving M2 macrophage
677 polarization mediated by hif-1αinduced IL-10. Oncoimmunology 2016;5:e1221557.
678 https://doi.org/10.1080/2162402X.2016.1221557.

679 [40] Mukai K, Miyagi T, Nishio K, Yokoyama Y, Yoshioka T, Saito Y, et al. S100A8 Production
680 in CXCR2-expressing CD11b + Gr-1 high cells aggravates hepatitis in mice fed a high-fat
681 and high-cholesterol Diet . J Immunol 2016;196:395–406.
682 https://doi.org/10.4049/jimmunol.1402709.

683 [41] Koliaki C, Szendroedi J, Kaul K, Jelenik T, Nowotny P, Jankowiak F, et al. Adaptation of
684 hepatic mitochondrial function in humans with non-alcoholic fatty liver is lost in
685 steatohepatitis. Cell Metab 2015;21:139–46.
686 https://doi.org/10.1016/j.cmet.2015.04.004.

687 [42] Gornicka A, Morris-Stiff G, Thapaliya S, Papouchado BG, Berk M, Feldstein AE.
688 Transcriptional profile of genes involved in oxidative stress and antioxidant defense in a
689 dietary murine model of steatohepatitis. Antioxidants Redox Signal 2011;15:437–45.
690 https://doi.org/10.1089/ars.2010.3815.

691 [43] Wang H, Liu Y, Wang D, Xu Y, Dong R, Yang Y, et al. The upstream pathway of mTOR-
692 mediated autophagy in liver diseases. Cells 2019;8: pii: E1597.
693 https://doi.org/10.3390/cells8121597.

694 [44] Lian J, Watts R, Quiroga AD, Beggs MR, Alexander RT, Lehner R. Ces1d deficiency
695 protects against high-sucrose diet-induced hepatic triacylglycerol accumulation. J Lipid
696 Res 2019;60:880–891. https://doi.org/10.1194/jlr.M092544.

697 [45] Tanaka S, Hikita H, Tatsumi T, Sakamori R, Nozaki Y, Sakane S, et al. Rubicon inhibits
698 autophagy and accelerates hepatocyte apoptosis and lipid accumulation in nonalcoholic
699 fatty liver disease in mice. Hepatology 2016;64:1994–2014.

700 https://doi.org/10.1002/hep.28820.

701 [46] Miyagawa K, Oe S, Honma Y, Izumi H, Baba R, Harada M. Lipid-induced endoplasmic
702 reticulum stress impairs selective autophagy at the step of autophagosome-lysosome
703 fusion in hepatocytes. Am J Pathol 2016;186:1861–1873.
704 https://doi.org/10.1016/j.ajpath.2016.03.003.

705 [47] Koga H, Kaushik S, Cuervo AM. Altered lipid content inhibits autophagic vesicular
706 fusion. FASEB J 2010;24:3052–65. https://doi.org/10.1096/fj.09-144519.

707 [48] Yang X, Wang J, Dai J, Shao J, Ma J, Chen C, et al. Autophagy protects against dasatinib-
708 induced hepatotoxicity via p38 signaling. Oncotarget 2015;6:6203–17.
709 https://doi.org/10.18632/oncotarget.3357.

710 [49] Liu J, Chang F, Li F, Fu H, Wang J, Zhang S, et al. Palmitate promotes autophagy and
711 apoptosis through ROS-dependent JNK and p38 MAPK. Biochem Biophys Res Commun
712 2015;463:262–7. https://doi.org/10.1016/j.bbrc.2015.05.042.

713 [50] Chen Y, Dorn GW. PINK1-phosphorylated mitofusin 2 is a parkin receptor for culling
714 damaged mitochondria. Science 2013;340:471–5.
715 https://doi.org/10.1126/science.1231031.

716 [51] Sebastián D, Hernández-Alvarez MI, Segalés J, Sorianello E, Muñoz JP, Sala D, et al.
717 Mitofusin 2 (Mfn2) links mitochondrial and endoplasmic reticulum function with insulin
718 signaling and is essential for normal glucose homeostasis. Proc Natl Acad Sci U S A
719 2012;109:5523–8. https://doi.org/10.1073/pnas.1108220109.

720 [52] Akundi RS, Huang Z, Eason J, Pandya JD, Zhi L, Cass WA, et al. Increased mitochondrial
721 calcium sensitivity and abnormal expression of innate immunity genes precede
722 dopaminergic defects in Pink1-deficient mice. PLoS One 2011;6:e16038.
723 https://doi.org/10.1371/journal.pone.0016038.

724 [53] Yamada T, Dawson TM, Yanagawa T, Iijima M, Sesaki H. SQSTM1/p62 promotes
725 mitochondrial ubiquitination independently of PINK1 and PRKN/parkin in mitophagy.
726 Autophagy 2019;15:2012–2018. https://doi.org/10.1080/15548627.2019.1643185.

727 [54] Lim JS, Mietus-Snyder M, Valente A, Schwarz JM, Lustig RH. The role of fructose in the
728 pathogenesis of NAFLD and the metabolic syndrome. Nat Rev Gastroenterol Hepatol
729 2010;7:251–64. https://doi.org/10.1038/nrgastro.2010.41.

730 [55] Simoes ICM, Janikiewicz J, Bauer J, Karkucinska-Wieckowska A, Kalinowski P. Dobrzyn A

731 et al. Fat and Sugar-A Dangerous Duet. A Comparative Review on Metabolic
732 Remodeling in Rodent Models of Nonalcoholic Fatty Liver Disease. Nutrients.
733 2019;11(12):2871. doi:10.3390/nu11122871

734

735 [56] Hu Y, Semova I, Sun X, Kang H, Chahar S, Hollenberg AN, et al. Fructose and glucose can
736 regulate mammalian target of rapamycin complex 1 and lipogenic gene expression via
737 distinct pathways. J Biol Chem 2018;293:2006–14.
738 https://doi.org/10.1074/jbc.M117.782557.

739 [57] Montgomery MK, Fiveash CE, Braude JP, Osborne B, Brown SHJ, Mitchell TW, et al.
740 Disparate metabolic response to fructose feeding between different mouse strains. Sci
741 Rep 2015;5:18474. https://doi.org/10.1038/srep18474.

742 [58] Gaude E, Schmidt C, Gammage PA, Dugourd A, Blacker T, Chew SP, et al. NADH
743 Shuttling Couples Cytosolic Reductive Carboxylation of Glutamine with Glycolysis in
744 Cells with Mitochondrial Dysfunction. Mol Cell 2018;69:581-593.
745 https://doi.org/10.1016/j.molcel.2018.01.034.

746 [59] Chen Q, Kirk K, Shurubor YI, Zhao D, Arreguin AJ, Shahi I, et al. Rewiring of glutamine
747 metabolism is a bioenergetic adaptation of human cells with mitochondrial DNA
748 mutations. Cell Metab 2018;27:1007–1025.
749 https://doi.org/10.1016/j.cmet.2018.03.002.

750 [60] Tang Y, Wallace M, Sanchez-Gurmaches J, Hsiao WY, Li H, Lee PL, et al. Adipose tissue
751 mTORC2 regulates ChREBP-driven de novo lipogenesis and hepatic glucose metabolism.
752 Nat Commun 2016:7:11365. https://doi.org/10.1038/ncomms11365.

753 [61] Cao H, Gerhold K, Mayers JR, Wiest MM, Watkins SM, Hotamisligil GS. Identification of
754 a lipokine, a lipid hormone linking adipose tissue to systemic metabolism. Cell
755 2008;134:933–44. https://doi.org/10.1016/j.cell.2008.07.048.

756 [62] Yore MM, Syed I, Moraes-Vieira PM, Zhang T, Herman MA, Homan EA, et al. Discovery
757 of a class of endogenous mammalian lipids with anti-diabetic and anti-inflammatory
758 effects. Cell 2014;159:318–32. https://doi.org/10.1016/j.cell.2014.09.035.

759 [63] Yew Tan C, Virtue S, Murfitt S, Robert LD, Phua YH, Dale M, et al. Adipose tissue fatty
760 acid chain length and mono-unsaturation increases with obesity and insulin resistance.
761 Sci Rep 2015;5:18366. https://doi.org/10.1038/srep18366.

762 [64] Thörne A, Lönnqvist F, Apelman J, Hellers G, Arner P. A pilot study of long-term effects
763 of a novel obesity treatment: Omentectomy in connection with adjustable gastric
764 banding. Int J Obes 2002;26:193–9. https://doi.org/10.1038/sj.ijo.0801871.

765 [65] Muzumdar R, Allison DB, Huffman DM, Ma X, Atzmon G, Einstein FH, et al. Visceral
766 adipose tissue modulates mammalian longevity. Aging Cell 2008;7:438–40.
767 https://doi.org/10.1111/j.1474-9726.2008.00391.x.

768 [66] Tran TT, Kahn CR. Transplantation of adipose tissue and stem cells: Role in metabolism
769 and disease. Nat Rev Endocrinol 2010;6:195–213.
770 https://doi.org/10.1038/nrendo.2010.20.

771 [67] Booth AD, Magnuson AM, Fouts J, Wei Y, Wang D, Pagliassotti MJ, et al. Subcutaneous
772 adipose tissue accumulation protects systemic glucose tolerance and muscle
773 metabolism. Adipocyte 2018;7:261–272.
774 https://doi.org/10.1080/21623945.2018.1525252.

775 [68] Cox-York K, Wei Y, Wang D, Pagliassotti MJ, Foster MT. Lower body adipose tissue
776 removal decreases glucose tolerance and insulin sensitivity in mice with exposure to
777 high fat diet. Adipocyte 2015;4:32–43.
778 https://doi.org/10.4161/21623945.2014.957988.

779 [69] Zhang Y, Wang H, Zhang L, Yuan Y, Yu D. Codonopsis lanceolata polysaccharide CLPS
780 alleviates high fat/high sucrose diet-induced insulin resistance via anti-oxidative stress.
781 Int J Biol Macromol 2019; pii: S0141-8130(19)35823-4.
782 https://doi.org/10.1016/j.ijbiomac.2019.09.185.

783 [70] Gaballah HH, El-Horany HE, Helal DS. Mitigative effects of the bioactive flavonol fisetin
784 on high-fat/high-sucrose induced nonalcoholic fatty liver disease in rats. J Cell Biochem
785 2019;120:12762–774. https://doi.org/10.1002/jcb.28544.

786 [71] Anhê FF, Nachbar RT, Varin T V., Vilela V, Dudonné S, Pilon G, et al. A polyphenol-rich
787 cranberry extract reverses insulin resistance and hepatic steatosis independently of
788 body weight loss. Mol Metab 2017;6:1563–73.
789 https://doi.org/10.1016/j.molmet.2017.10.003.

790 [72] Chu MJJ, Hickey AJR, Jiang Y, Petzer A, Bartlett ASJR, Phillips ARJ. Mitochondrial
791 dysfunction in steatotic rat livers occurs because a defect in complex i makes the liver
792 susceptible to prolonged cold ischemia. Liver Transplant 2015;21:396–407.

793 https://doi.org/10.1002/lt.24024.

794 [73] Milton-Laskibar I, Aguirre L, Etxeberria U, Milagro FI, Martínez JA, Portillo MP.
795 Involvement of autophagy in the beneficial effects of resveratrol in hepatic steatosis
796 treatment. A comparison with energy restriction. Food Funct 2018;9:4207–15.
797 https://doi.org/10.1039/c8fo00930a.

798 [74] Sun Y, Xia M, Yan H, Han Y, Zhang F, Hu Z, et al. Berberine attenuates hepatic steatosis
799 and enhances energy expenditure in mice by inducing autophagy and fibroblast growth
800 factor 21. Br J Pharmacol 2018;175:374–87. https://doi.org/10.1111/bph.14079.

801 [75] Hemmings BA, Restuccia DF. PI3K-PKB/Akt pathway. Cold Spring Harb Perspect Biol
802 2012;4:a011189. https://doi.org/10.1101/cshperspect.a011189.

803 **FIGURE LEGENDS**

804

805 **Fig. 1. High-fat high-sucrose diet promotes steatohepatitis.** Changes in body weight
806 (A), cumulative food intake (B), energy intake (C), biochemical parameters (D), liver
807 weight and histological variables (E and F) in mice fed with a chow diet (CD), high-fat
808 diet (HFD) or high-fat high sucrose diet (HF-HSD). Results are shown as means and
809 standard error of the mean. *p<0.05, **p<0.01, ***p<0.001; NAS: Non-alcoholic fatty
810 liver activity score

811

812 **Fig. 2. High-fat high-sucrose diet increases hepatic oxidative stress.**
813 Immunohistochemical analyses (A) enzyme activity assays (B), and immunoblotting
814 analyses (C) of oxidative stress markers and antioxidant enzymes in mice fed with a
815 chow diet (CD), high-fat diet (HFD) or high-fat high-sucrose diet (HF-HSD). Results are
816 shown as means and standard error of the mean; *p<0.05, **p<0.01

817

818 **Fig. 3. Loss of hepatic metabolic adaptation in mice with steatohepatitis.** .
819 Immunoblotting analyses (A) of mitochondrial complexes, and key proteins involved in
820 the *de novo* lipogenic pathway and expression of mitochondrial and cytosolic genes (B)
821 in mice fed with a chow diet (CD), high-fat diet (HFD) or high-fat high-sucrose diet (HF-
822 HSD). Results are shown as means and standard error of the mean; *p < 0.05.
823 ACC: acetyl-CoA carboxylase; ACLY: ATP-citrate lyase; IDH 1: Isocitrate dehydrogenase
824 1; IDH 2: Isocitrate dehydrogenase 2; FAH: fumarylacetoacetate hydrolase; FASN, fatty
825 acid synthase; OGDH: Oxoglutarate dehydrogenase; SDHA: succinate dehydrogenase.
826 The other parameters analyzed in (A) are different complexes of oxidative
827 phosphorylation.

828

829 **Fig. 4. High-fat high-sucrose diet induces mitophagy defects**. ((A) Immunoblotting
830 analyses of autophagy and mitophagy components. Results are shown as means and
831 standard error of the mean; *p<0.05
832 AMPK: AMP-activated protein kinase; ATG7: autophagy-related protein 7; LC3:
833 microtubule-associated proteins 1A/1B light chain 3; MFN2: mitofusin 2; MAPK:

834 mitogen activated protein kinase; mTOR: mammalian target of rapamycin; P62:
835 sequestosome 1; PARKIN: E3 ubiquitin- protein ligase parkin; PINK1: PTEN-induced
836 putative kinase 1; TOM20: translocase outer membrane 20.
837
838 **Fig. 5. The loss of adipose tissue dynamics is associated with an increase in adipocyte**
839 **size**. (A to C): Histological analyses of perigonadal white adipose tissue (pgWAT) and
840 inguinal white adipose tissue (iWAT) were performed to determine the adipocyte size.
841 (D): Immunoblotting analyses of proteins regulating lipolysis, lipogenesis, and
842 mitochondrial status. Results are shown as means and standard error of the mean;
843 *p<0.01, **p<0.001
844 ACC: acetyl-CoA carboxylase; AMPK: AMP-activated protein kinase; FAH:
845 fumarylacetoacetate hydrolase; FASN, fatty acid synthase; HSL, hormone sensitive
846 lipase; TOM20: translocase outer membrane 20; UCP-1, uncoupling protein 1. The
847 other parameters analyzed in (D) are different complexes of oxidative phosphorylation
848
849 **Fig. 6. Changes in the levels of lipid species in perigonadal adipose tissue linked to**
850 **the high-fat high-sucrose diet**. Graphical representation of the acetyl-CoA metabolism
851 focusing on β-oxidation and the synthesis of fatty acid, bile acids, steroid, and
852 phospholipids
853 CA: acid cholic; CDCA; chenodeoxycholic acid; DAG: diacilglicerol; DCA: deoxycholic
854 acid; GCA: glycocholic acid; GCDCA: glycochenodeoxycholic acid; GLCA:
855 glycolithocholate acid; GDCA: glycodeoxycholic acid; GUDCA: glycoursodeoxycholic
856 acid; G3P: glycerol-3-phosphate; LPA: lysophosphatidic acid; LPS:
857 lysophosphatidylserine; PA: phosphatidic acid; TCA: taurocholic acid; TCDCA:
858 taurochenodeoxycholic acid; lithocholic acid; TDCA: taurodeoxycholic acid; TLCA:
859 taurolithocholic acid; TUDCA; tauroursodeoxycholic acid.
860

Figure 1

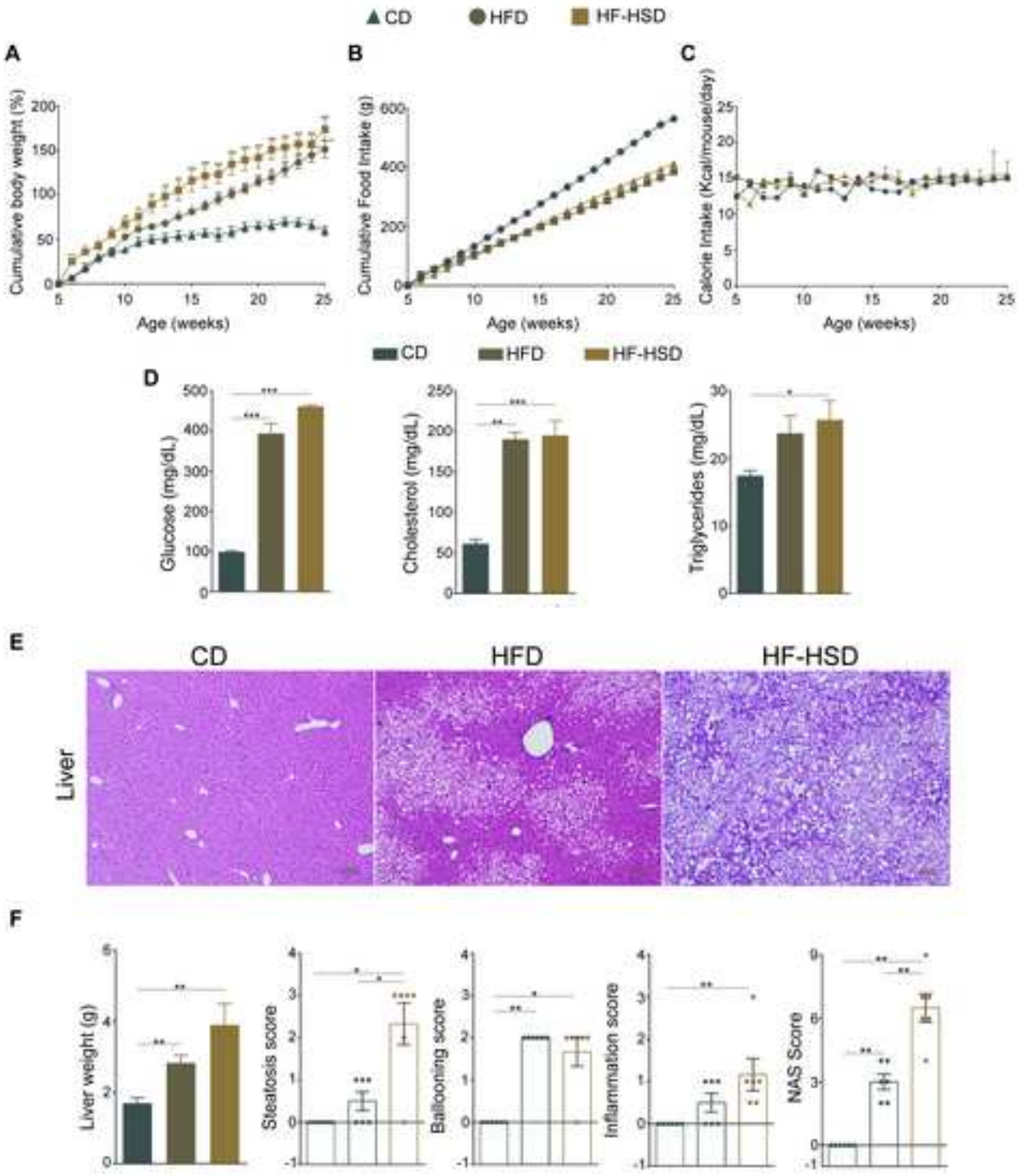

Figure 2

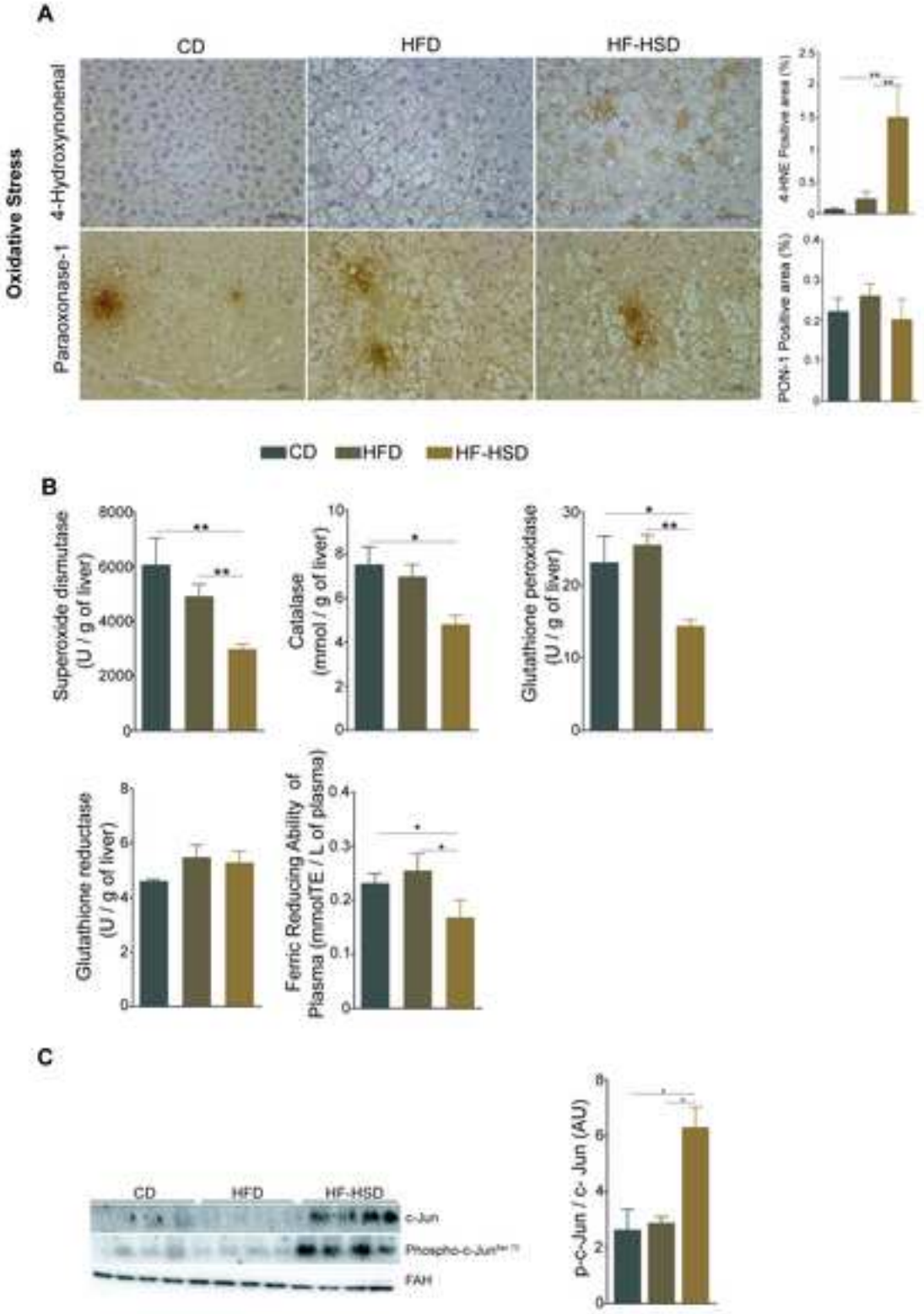

Figure 3

Click here to access/download;Figure;Figure 3.jpg

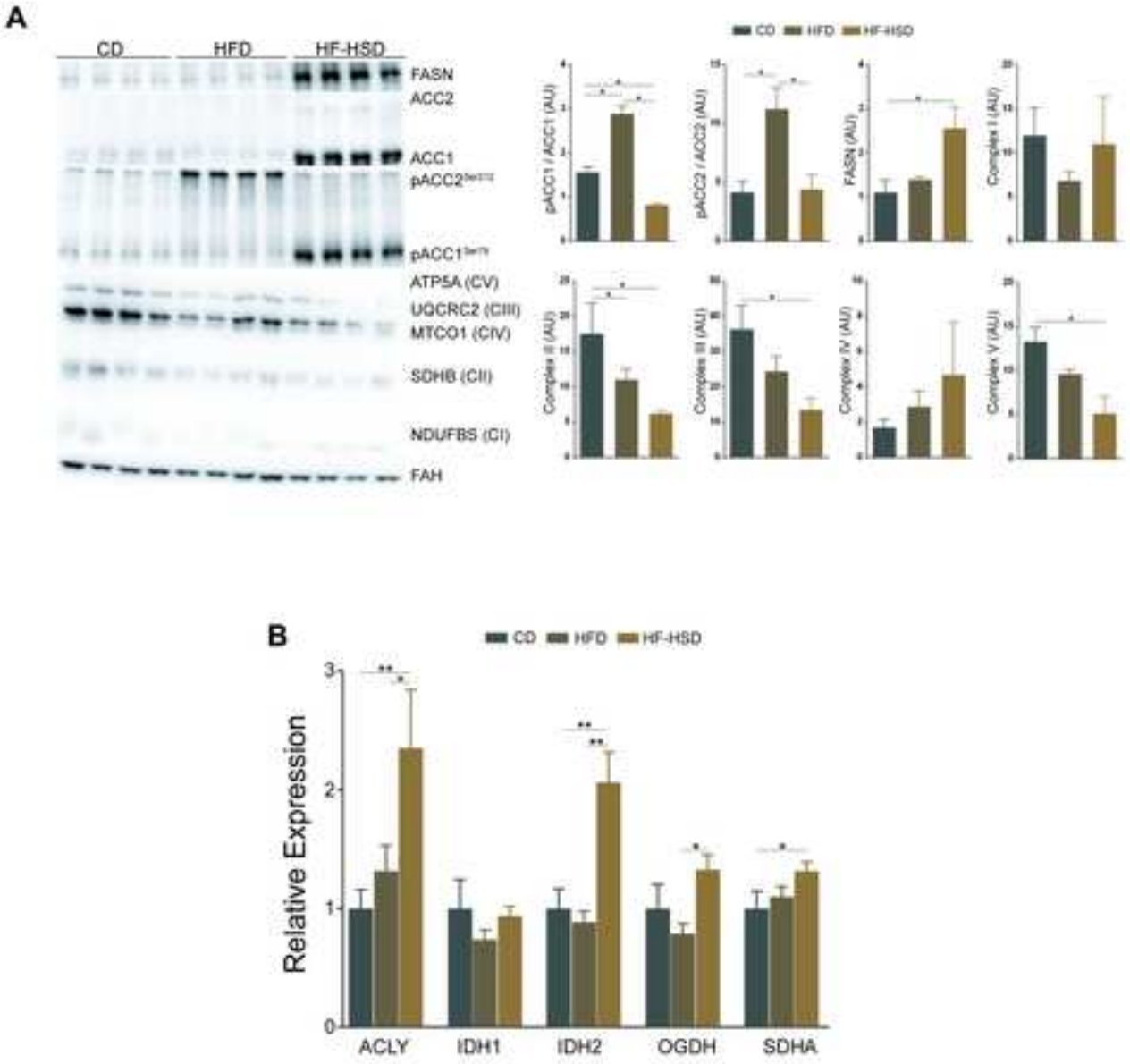

Figure 4

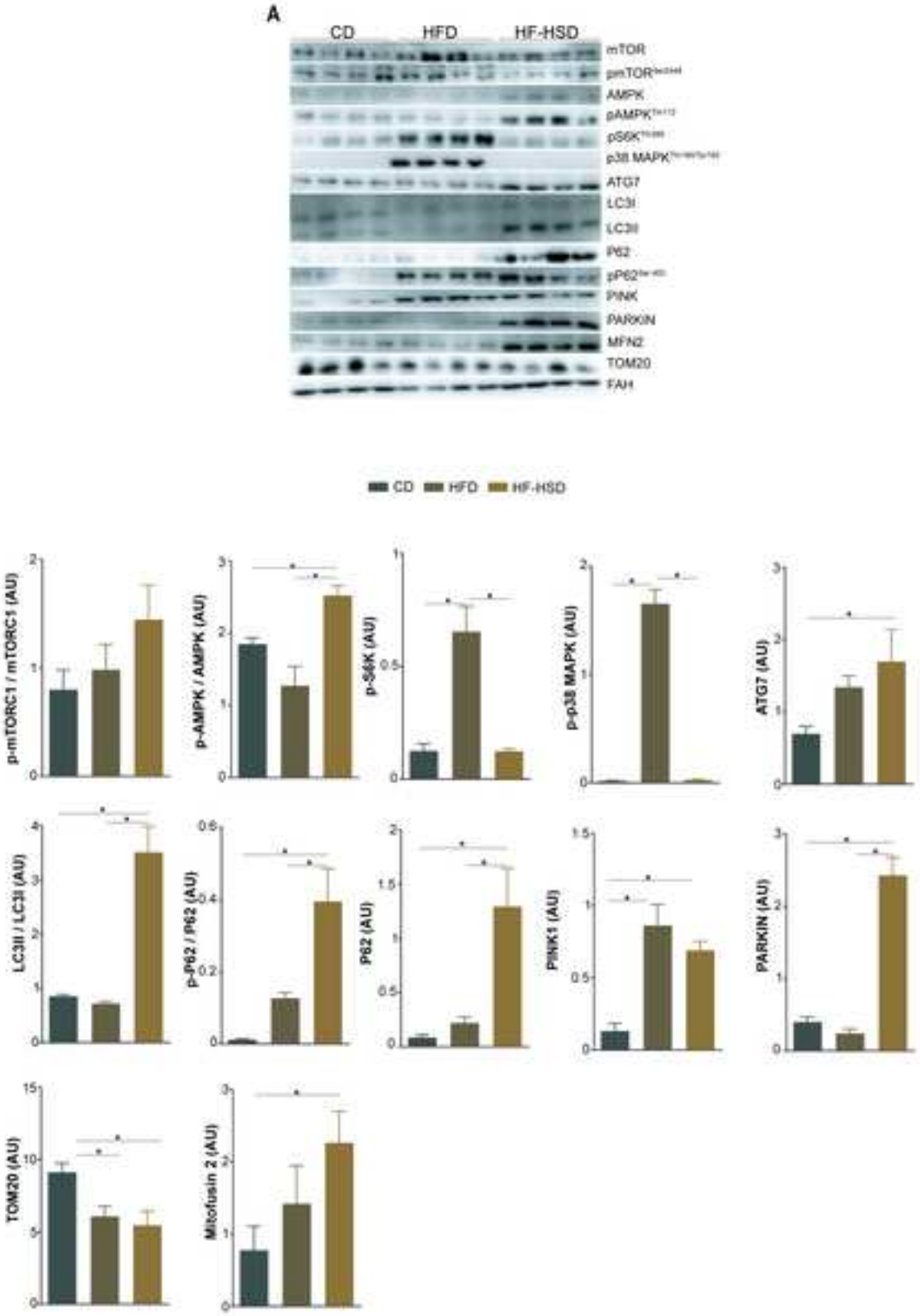

Figure 5

Click here to access/download;Figure;Figure 5.jpg

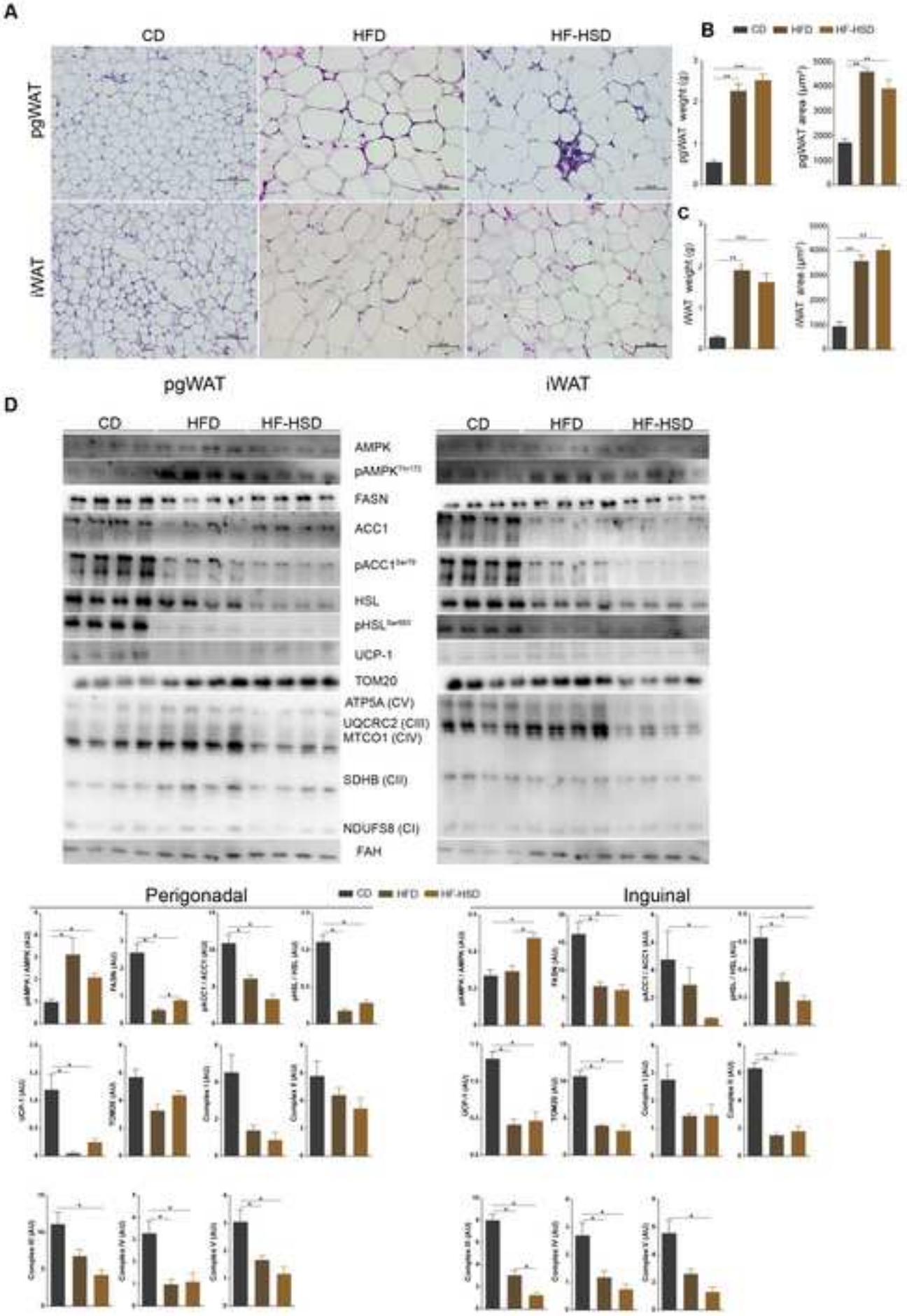

Figure 6

Click here to access/download;Figure;Figure 6.jpg

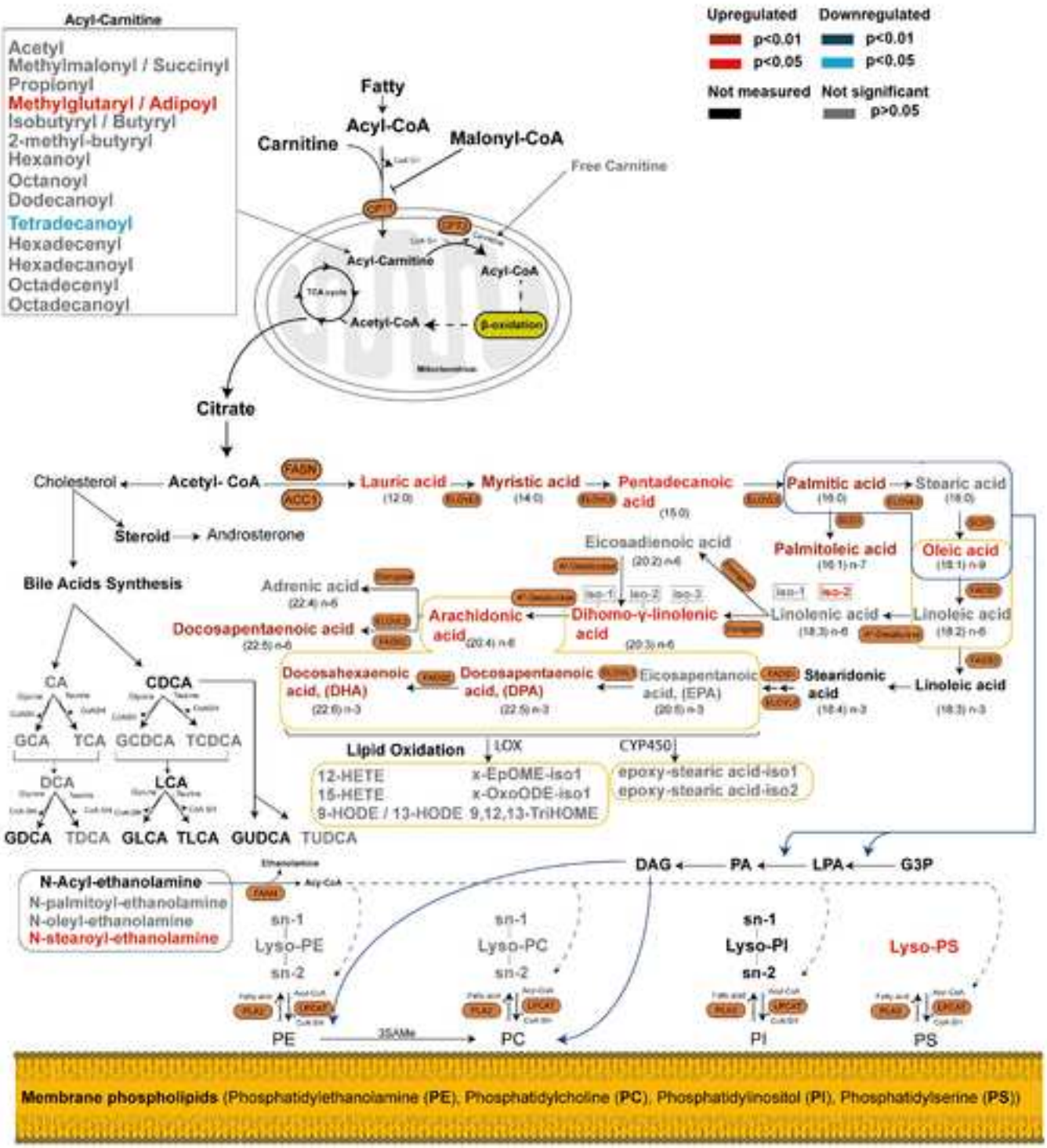

Author contributions

Gerard Baiges-Gaya, Jordi Camps, Jorge Joven: Conceptualization; Gerard Baiges-Gaya, Jordi Camps: Data curation; Gerard Baiges-Gaya, Jordi Camps, Jorge Joven: Formal analysis; Marta Romeu, Maria-Rosa Nogués, Jorge Joven: Funding acquisition; Gerard Baiges-Gaya, Salvador Fernández-Arroyo, Fedra Luciano-Mateo, Noemí Cabré, Elisabet Rodríguez-Tomàs, Anna Hernández-Aguilera, Helena Castañé: Investigation; Gerard Baiges-Gaya, Salvador Fernández-Arroyo, Fedra Luciano-Mateo, Noemí Cabré, Elisabet Rodríguez-Tomàs, Anna Hernández-Aguilera, Helena Castañé: Methodology; Jordi Camps, Jorge Joven: Project administration; Salvador Fernández-Arroyo, Marta Romeu, Maria-Rosa Nogués, Jorge Joven: Resources; Gerard Baiges-Gaya, Salvador Fernández-Arroyo: Software; Jordi Camps, Jorge Joven: Supervision; Gerard Baiges-Gaya, Jordi Camps, Jorge Joven: Validation; Jordi Camps: Visualization; Gerard Baiges-Gaya: Writing – original draft; Jordi Camps: Writing – review & editing.